HORIZON 2020

THEME SC5-2017

(Grant Agreement 776613)

European Climate Prediction system (EUCP)

Deliverable D4.4

Case studies and events of interest: Lessons learned and future opportunities

Deliverable Title	*Case studies and events of interest: Lessons learned and future opportunities*	
Brief Description	*This deliverable provides an array of cases studies and events of interest from the EUCP project, used in the WP #4 (title - end user driven characterisation of near term trends in regional climate impact and risks) for testing the developed EUCP data and methodologies in sectoral applications in connection with stakeholders. The list of cases also includes potential cases envisaged in future applications. The cases developed here are concerning several sectors: energy, infrastructure, agriculture and water sectors, but are also of interest for local, regional and national authorities. We list cases but also focus on technical usability and value of the new datasets and methods.*	
WP number	*WP4*	
Lead Beneficiary	*Robert Vautard, CNRS-IPSL*	
Contributors	*Shuang Yu, CNRS-IPSL* *Robert Vautard, CNRS-IPSL* *Carlos Delgado-Torres, BSC* *Albert Soret, BSC* *Balakrishnan Solaraju-Murali, BSC* *Frederiek Sperna Weiland, DELTARES* *Peter Greve, IIASA*	
Creation Date Version Number Version Date	*29/05/2022* *version 2.0* *29/05/2022*	
Deliverable Due Date Actual Delivery Date	*31/05/2022* *31/05/2022*	
Nature of the Deliverable	R	*R – Report*
		P - Prototype
		D - Demonstrator
		O - Other
Dissemination Level/ Audience	*PU*	*PU - Public*
		PP - Restricted to other programme participants, including the Commission services
		RE - Restricted to a group specified by the consortium, including the Commission services
		CO - Confidential, only for members of the consortium, including the Commission services

Version	Date	Modified by	Comments
1.0	29/05/2022	Robert Vautard, CNRS-IPSL	Carol McSweeney, Met office Jason Lowe, Met office
2.0	31/05/2022	Jason Lowe	Final review

Table of contents

1. Executive Summary..5
2. Project Objectives.. 5
3. Detailed Report... 6
3.1 Case #1: Wind energy drought in Brittany.
3.2 Case #2: Winter wind energy drought risk across Europe.
3.3 Case #3: Wind energy drought under cold conditions.
3.4 Case #4: Improved wind power assessment for high-resolution climate models in complex terrain (Southern France).
3.5 Case #5: Wind drought in Eastern USA.
3.6 Case #6: Pluvial flood hazard and risk in Milan.
3.7 Case #7: Extreme sea levels along Upper Adriatic Sea coasts.
3.8 Case #8: Multi-year prediction of dry conditions over global wheat harvesting regions.
3.9 Case #9: Water use impact simulations and projections under 2K global warming.
3.10 Case #10: Future changes in hurricane occurrence in the Caribbean.
3.11 Case #11: Urban and flash flooding.
3.12 List peer reviewed articles.
3.13 List planned future publications.
4. Lessons Learnt and links built.. 46
5. References... 48

List of Tables

Table 3.1: List of remarkable cases used in EUCP.. 52

List of Figures

Figure 3.1: Seasonal cycle of surface wind based on observations during 1988-2017........ 52

EUCP
European Climate Prediction system

1. Executive summary

This deliverable provides an array of cases studies and events of interest from the EUCP project, used in the WP #4 - end user-driven analysis of future climate risks and potential impacts, for testing the developed EUCP data and methodologies in sectoral applications in connection with stakeholders. The list of cases also includes potential cases envisaged in future applications. The cases developed here are concerning several sectors: energy, infrastructure, agriculture and water sectors, but are also of interest for local, regional and national authorities. We list cases but also focus on technical usability and value of the new datasets and methods. The case studies are not designed to cover all sectors of interest, and the lack of case studies in particular areas should not be considered as evidence of adaptation challenge in those sectors.

The deliverable is organized into (i) a summarizing table for the concerned cases, (ii) a set of 11 separated cases fact sheets for specific cases or applications. Each case is motivated by a specific question from stakeholders, which can vary from local authorities, industries. The question can concern one region or the entire Europe, and one specific type of event, *climatic impact driver* (following IPCC AR6 WGI definition), or type of use of climatic information.

2. Project objectives

These deliverables have contributed to the following EUCP objectives (Description of Action, Section 1.1):

No.	Objective	Yes	No
1	Develop an ensembles climate prediction system based on high-resolution climate models for the European region for the near-term (~1-40 years)		No
2	Use the climate prediction system to produce consistent, authoritative and actionable climate information	Yes	
3	Demonstrate the value of this climate prediction system through high impact extreme weather events in the near past and near future	Yes	
4	Develop, and publish, methodologies, good practice and guidance for producing and using EUCP's authoritative climate predictions for 1-40 year timescales	Yes	

3. Detailed report

The list of case studies is summarized in Table 3.1 below. In each case we describe the sector, the practical challenge and questions to be answered, requiring data and methodologies from EUCP, the type of data and methods needed, and a remark regarding the (witnessed or anticipated) success of the application, the challenges. Details are then provided in fact sheets (sections 3.1 - 3.11).

Overall, all cases showed benefits from increased ensemble size and increased resolution of the climate models used, whether they are long-term climate projections or decadal predictions. In some of the mentioned cases, results are still preliminary. In most cases also, the limited length of series generated by models for high-resolution scenarios is problematic making it difficult to ensure good statistics, but show promising results. Also, decadal predictions lack high resolution model simulations currently. All these cases advocate for a general continuation of the EUCP modeling work, and show the good improvement in information for adaptation.

Table 3.1. list of remarkable cases used in EUCP.

Case #, title	Sector / user	challenge	Data	methods	remarks
1: Wind droughts in Brittany	Local wind energy producer	Determine if wind droughts frequency changes up to today and wind energy potential are decreasing at a local site, to estimate revenue adjustment relative to test period	Regional climate projections	Ensemble statistics, attribution	**Success** : requirement of model ensemble for extreme statistics **Challenges** : very high resolution not long enough for extreme statistics **Improvement potential**: use of ensemble weighting methods from WP2, enlarge model ensemble to improve statistics
2: Wind droughts at European scales	large-scale wind energy producer, transmission network	Determine probability of future energy revenue deficits in long periods such as a full winter season for a large-scale producer; determine most constraining events for future energy mix scenario	Regional climate projections	Ensemble statistics, attribution	**Success** : requirement of large ensemble for extreme statistics **Challenges** : very high resolution not long enough for extreme statistics **Improvement potential**: use of ensemble weighting methods from WP2, enlarge model ensemble to improve statistics
3: Compound cold spell and wind drought	Transmission network	Determine probability of compound event with cold and lack of wind which requires a lot of back up production	Regional climate projections	Ensemble statistics, attribution	**Success** : requirement of large ensemble for extreme statistics **Challenges** : accurate representation in atmospheric dynamics, winds

Case #, title	Sector / user	challenge	Data	methods	remarks
					Improvement potential: use of ensemble weighting methods from WP2, enlarge model ensemble to improve statistics
4: Improved wind power assessment from very high-resolution model	Wind energy producer	Capture the correct wind variability at local, near-site scale, with long-term statistics	WP3 high-resolution climate projections	Simple statistics, model intercomparison	**Success** : clear difference from high to very high resolution in complex terrain **Challenges** : lack of observations to evaluate models, not enough data to assess distributions **Improvement potential**: enlarge model ensemble to improve statistics, provide longer simulations at very high resolution
5: Wind drought in Eastern USA	Wind energy	Predict surface wind speed at multi-annual and multi-seasonal time scales	CMIP6/DCPP-A and CMIP/DCPP-B	Multi-model ensemble. Skill assessment	**Success**: Use of some of the DCPP simulations which have been performed within EUCP WP1 **Challenges**: identify regions of significant skill, collect enough model data to ensure robust statistics
6: Pluvial flood hazard and risk in Milan	Water management	Assess cost/benefits of adaptation scenarios, using in particular nature-based solutions	EUCP WP3 CP simulations+cost/benefit economic approach	Extreme value statistics pluvial inundation modelling benefits of nature-based solutions	**Success**: high resolution, convection permitting simulations allow to refine the pluvial flood hazard and risk - and assess performance of nature-based solutions **Challenges**: simulation of risk reduction measures and planning of urban green areas challenging in densely developed areas
7: Extreme sea levels along Upper Adriatic Sea coasts	Infrastructure & water management	Assess cost/benefits of adaptation scenarios of defence infrastructures for extreme sea levels	CMIP5+SLR model and inundation model Cost/benefit approach	Extreme value statistics, coastal inundation modeling, nature-based solutions - performance	**Success**: risk modeling chain + economic assessment framework developed and applied to inform local adaptation efforts **Challenges**: modeling requires high resolution DEM - vertical elevation errors have potential to underestimate/ overestimate the coastal flood hazards and

Case #, title	Sector / user	challenge	Data	methods	remarks
					misguide the adaptation measure
8: Multi-year prediction of dry conditions over global wheat harvesting regions	Agriculture	Predict the evolution of multi-year drought condition during the six months previous to the wheat harvesting month globally	CMIP6/DCPP-A and CMIP/DCPP-B	Multi-model ensemble, Bias adjustment, Skill assessment	**Success**: application of EUCP decadal forecasts, design of a quite general method applicable to more crops **Challenges**: ensemble member numbers currently too limited to grant significant and reliable forecasts
9: Water use impact simulations and projections under 2K global warming.	Water	Assess the sensitivity of low flow projections to changes in water use under climate change conditions	WP2 pseudo-global warming projections	Hydrological impact simulations	**Success**: Using a new hydrological impact model from IIASA partly developed within EUCP
10: Future changes in hurricane occurrence in the Caribbean	Water / flooding	Assess the potential future change in hurricane occurrence and impact over the Caribbean Islands (outermost regions of the EU)	WP2 / 3: High-resolution global warming projections KNMI	Coastal, hydrological and flood modelling + hurricane track analysis	**Success** : Access to high-resolution climate data for Caribbean **Challenges** : Although it is a PGW experiment the hurricane tracks do slightly change and there are only a limited number of hurricanes to investigate
11: Urban and flash flooding	Water / flooding	Assess change in future urban and future flash flooding	WP3: CP-RCM simulations	Statistical analysis + hydrological modelling	**Success** : Use of the ensemble of CP-RCM datasets developed in WP3 for hydrological impact analysis **Challenges** : Limited CP-RCM time-series length hamper extreme value analysis **Improvement potential**: Longer CP-RCM time-series or advanced statistical analysis.

In the remarks column of the table, the success is something that has been achieved, and the challenges is the limitations of research, and the improvement potential is the description of possible improvement in the future.

3.1 Case #1: Wind energy drought in Brittany.

3.1.1 Practical question posed by stakeholders

Wind power, an important substituent for conventional fuels, may be challenged by reduction of surface wind speed in many regions of the word, which have been occurring over land in the last 30-50 years, a phenomenon known as global terrestrial wind stilling (Roderick et al., 2007; Vautard et al., 2010). Brittany has several wind farms. Based on observations from one of the sites, the surface wind speed has remained stable from 1988-2007 and there was no significant trend during this period (Fig.3.1). However, since 2008, the wind speed dropped sharply and has never rebounded to the original level, which caused large wind energy production losses in Brittany. As the occurrence of wind drought receives increasing attention, two questions were asked by the local wind energy producer. Will the decrease in wind energy resources continue in the future? Are the current wind energy drought caused by climate change?

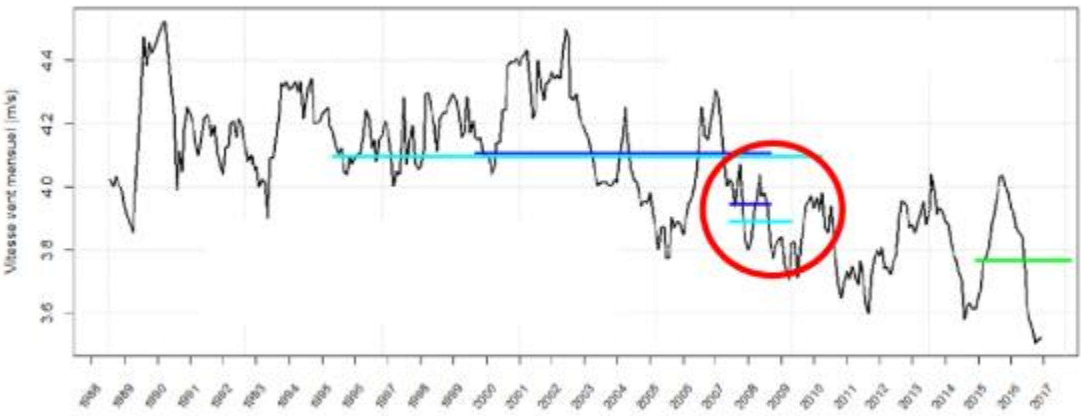

Fig.3.1. Seasonal cycle of surface wind based on observations during 1988-2017. The operational period (green) wind weaker than assessment period (blue).

3.1.2 General strategy used to solve the question

The challenges to overcome of this study are to determine if wind droughts frequency changes up to today and wind energy potential are decreasing at a local site, and to estimate revenue adjustment relative to test period. We consider here only the climate question. For this, we use the attribution techniques. It could be used to examine whether human influence could impact extreme climate events at different scale (Stott et al., 2016). It starts from the choice of which events to analyze and proceeds with the event definition, observational analysis, model evaluation, multi-model multi-method attribution, hazard synthesis, vulnerability and exposure analysis and ends with the communication procedures (Philip et al., 2020).

3.1.3 Data and Methods

The area selected for this study is from -4.5 °W, 47.6°N and -1.5°W, 48°N. We used 10 high-resolution climate projections from the EURO-Cordex ensemble (Jacob et al., 2014) as a preliminary methodological test, which can then be continued with WP3 when ensembles will be long enough to carry out attribution. For these ensembles, natural forcing simulations were not available, but anthropogenic forcing from greenhouse gases was assumed dominant in explaining the differences between two climate periods during 1971-2000 and 2000-2029. We compared the extreme distribution from three time periods (1971-2000, previous; 2000-2029, current; and 2041-2069, future) to analyze the effect of anthropogenic impact on low wind energy events. The all forcing projections (2006-2100) under Representative Concentration Pathways (RCPs), RCP8.5 were used. Load factor (Bansal et al., 2002) was used to characterize wind energy in Brittany, which is calculated based on the 100m wind speed in WP4.3.

The indicator used here to describe wind energy stagnation was the minimum regional mean Load Factor in each winter (December-February), as most of revenue is expected to come from the winter period. The attribution of the extreme event consists in comparing probabilities of the indicator exceeds the threshold in different climate periods. For model ensemble, a nonparametric approach was used by pooling all indicator of each ensemble member into a single pool and computing the probability by counting the number of exceedances of the threshold.

3.1.4 Results and discussion

We use each model ensemble separately to estimate how human influence has altered the risk of load factor lower than the threshold. In the EURO-CORDEX ensemble, the threshold of ~10 years events of load factor is about 0.09. Load factor lower than threshold becomes more than 1.30 times as probable in the current climate than in the 1979-2000 climate [risk ratio=(1.03, 1.65)]. For the future period, actual and future simulations do not show much difference in the extreme low wind energy events [risk ratio=(0.89, 1.40)], despite a systematically higher probability in the future than in the actual simulations for low wind energy events.

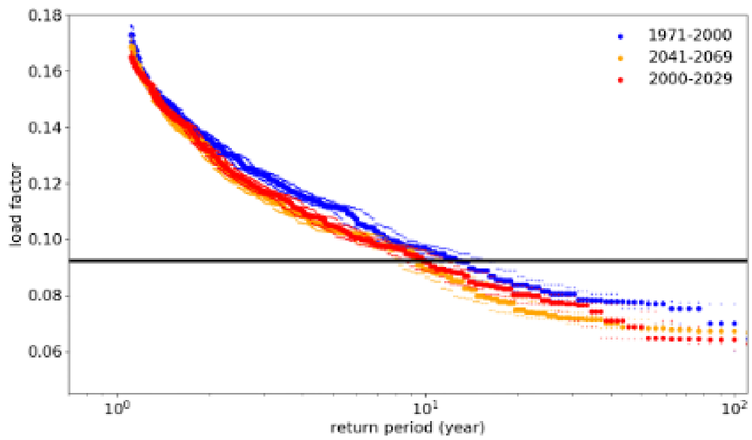

Fig.3.2. Changes in return values and return periods of load factor for model ensemble. The black horizontal line shows the return value corresponding to the 10-years return period during 2000 to 2029. Dots represent median of consecutive sorted return period/values model values from 10000 bootstrap estimations, together with 5%-95% confidence intervals (dashed lines).

Climate simulation suggests a slight potential increase in frequency of wind energy drought from the previous to the current climate, which is consistent, but with lower amplitude, with the wind stilling during the last 30-50 years over mid-latitude terrestrial surfaces (McVicar et al., 2012). In the future, the reduction of wind energy would not be significant compared with the current climate, but the wind energy production from Brittany will hardly return to its levels in the previous climate within the next 50 years.

Large ensemble for the model simulation is essential for extreme statistics and attribution research. The ensemble weight method from WP2 could be used in the next step to improve the accuracy of extreme statistics. In particular the adaptation of such methods to attribution, which has taken steps forward, e.g., with the work of Ribes et al. (2021), by adding observational constraints. In addition, the high-resolution climate model simulation might contribute to give credible projection of future wind energy drought at a local site. High-resolution climate models also hold promise but simulations are currently not long enough for the extreme statistics, which challenges the attribution research at a wind farm site. Thus, it is crucial to explore the long-term high-resolution climate simulations in future research.

References

Bansal, R. C., Bhatti, T. S., & Kothari, D. P. (2002). On some of the design aspects of wind energy conversion systems. *Energy conversion and management*, *43*(16), 2175-2187.

Efron, B., & Tibshirani, R. J. (1994). An introduction to the bootstrap. CRC press.

Jacob, D., and Coauthors, (2014): EURO-CORDEX: New high-resolution climate change projections for European impact research. Reg. Environ. Change, 14, 563–578, doi:10.1007/s10113-013-0499-2.

McVicar TR, Roderick ML, Donohue RJ, Li LT, Van Niel TG, Thomas A, Grieser J, Jhajharia D, Himri Y, Mahowald NM, Mescherskaya AV, Kruger AC, Rehman S, Dinpashoh Y. (2012). Global review and synthesis of trends in observed terrestrial near-surface wind speeds: implications for evaporation. J. Hydrol. 416–417: 182–205. https://doi.org/10.1016/j.jhydrol.2011.10.024.

Philip, S., Kew, S., van Oldenborgh, G. J., Otto, F., Vautard, R., van der Wiel, K., ... & van Aalst, M. (2020). A protocol for probabilistic extreme event attribution analyses. Advances in Statistical Climatology, Meteorology and Oceanography, 6(2), 177-203.

Ribes, A., Boé, J., Qasmi, S., Dubuisson, B., Douville, H., & Terray, L. (2022). An updated assessment of past and future warming over France based on a regional observational constraint. Earth System Dynamics Discussions, 1-29.

Roderick ML, Rotstayn LD, Farquhar GD, Hobbins MT. (2007). On the attribution of changing pan evaporation. Geophys. Res. Lett. 34(17): L17403.

Stott, P. A., Christidis, N., Otto, F. E., Sun, Y., Vanderlinden, J. P., van Oldenborgh, G. J., ... & Zwiers, F. W. (2016). Attribution of extreme weather and climate-related events. Wiley Interdisciplinary Reviews: Climate Change, 7(1), 23-41.

Vautard R, Cattiaux J, Yiou P, Thépaut JN, Ciais P. (2010). Northern hemisphere atmospheric stilling partly attributed to an increase in surface roughness. Nat. Geosci. 3(11): 756–761. https://doi.org/10.1038/ngeo979.

3.2 Case #2: Winter wind energy drought risk across Europe.

3.2.1 Practical question posed by stakeholders

As variable renewable energies are developing, wind energy is expected to play a crucial role as a mainstream source of electricity (DNV, 2018). The decline of wind speed in many regions of the world is expected to decrease wind power production, as wind speed is the most effective factor for comprehensive wind resource assessment (Jang and Byon, 2020). However, wind speed changes remain large discrepancies in space and time. Large-scale wind producers may have assets across Europe, with the impact of large-scale wind droughts on revenues. Beyond, such events may be important to account in future scenarios to anticipate large-scale energy back-up. Therefore, the question of concern for large-scale wind producers is whether there is significant spatial and temporal variability and changes of wind energy drought risk in different countries in Europe? And what about the changes in the future?

3.2.2 General strategy used to solve the question

Attribution of extreme climate events can be used to study changes that occurred for certain classes of events with specific magnitude, spatial scale, and timescale. In order to give numerical results actionable by stakeholders, the probability ratio (refers as risk ratio $=p_1/p_0$) was calculated to determine whether the frequency of a class of extremes is changing due to anthropogenic climate change (Philip et al., 2020). p1 is the probability of an event as strong as or stronger than the extreme event in the current climate and p0 is the probability in a counterfactual climate without anthropogenic emissions. The probability-based approach can potentially complement climate projections and therefore be useful for decision makers, who want a robust assessment of how event frequencies are changing for planning purposes, often based on specific thresholds.

3.2.3 Data and Methods

The area selected for this study comprises most of the land in Europe, bounded by -22°W, 33°S and 45.5°W, 72.5°N. The gridded dataset was taken from the ECMWF Reanalysis v5 (ERA5) for the period from 1979 to 2018 with a spatial resolution of 0.25°×0.25° (Hersbach et al., 2020), which was used in this study to estimate the observed trends in hub-height wind speed as its convincing performance in Europe (Jourdier, 2020). In this study, we used 10 high-resolution climate projections from the EURO-CORDEX (Coordinated Regional Climate Downscaling Experiment) ensemble (Jacob et al., 2014), with 4 Global climate Models downscaled by 4 Regional Climate Models. The all forcing projections (2006-2100) under Representative Concentration Pathways (RCPs), RCP8.5 were used.

The indicator used here to describe wind energy stagnation was the minimum monthly mean Load Factor (MLF) in each winter (December-February). Once the indicator is defined, a threshold was calculated as the return value of MLF corresponding to the 10-year return period in the current climate (2000-2029). The probability of MLF lower than the threshold could be calculated in the three different periods. For more quantitative results, the risk ratio was calculated to indicate the different probabilities of the wind energy drought between two climate periods. When the risk ratio <1, the low wind energy winter is more frequent in the earlier climate period.

3.2.4 Results and discussion

The risk ratios were calculated in each country during different climate periods. Fig.3.3 a, b show the regional differences of the return values of 10-year events during 2000-2029. Threshold increased smoothly from south to east with the largest difference in the United Kingdom. It means that as latitude increases, low wind energy load factors become larger. Fig.3.3 c, d show the risk ratios between current and previous periods in different countries. The results illustrate that the low wind energy winter occurred more frequently during 2000-2029 in most European countries. Coastal countries such as Norway, Italy and the United Kingdom have a higher risk ratio, as the increase in low wind energy winter frequency is even more remarkable. In addition, for few countries, such as Luxembourg, Moldova, Belgium, risk ratios are lower than 1 in part samplings. Compared with the current period, low wind energy winter occurs more frequently in the future in most countries as well (Fig.3.3 e, f), but the probability of occurrence in some countries is decreased, especially in most countries in the south and central Europe, such as Italy, Czech, Slovakia, Moldova, Hungary, Austria, Slovenia, Romania, etc.

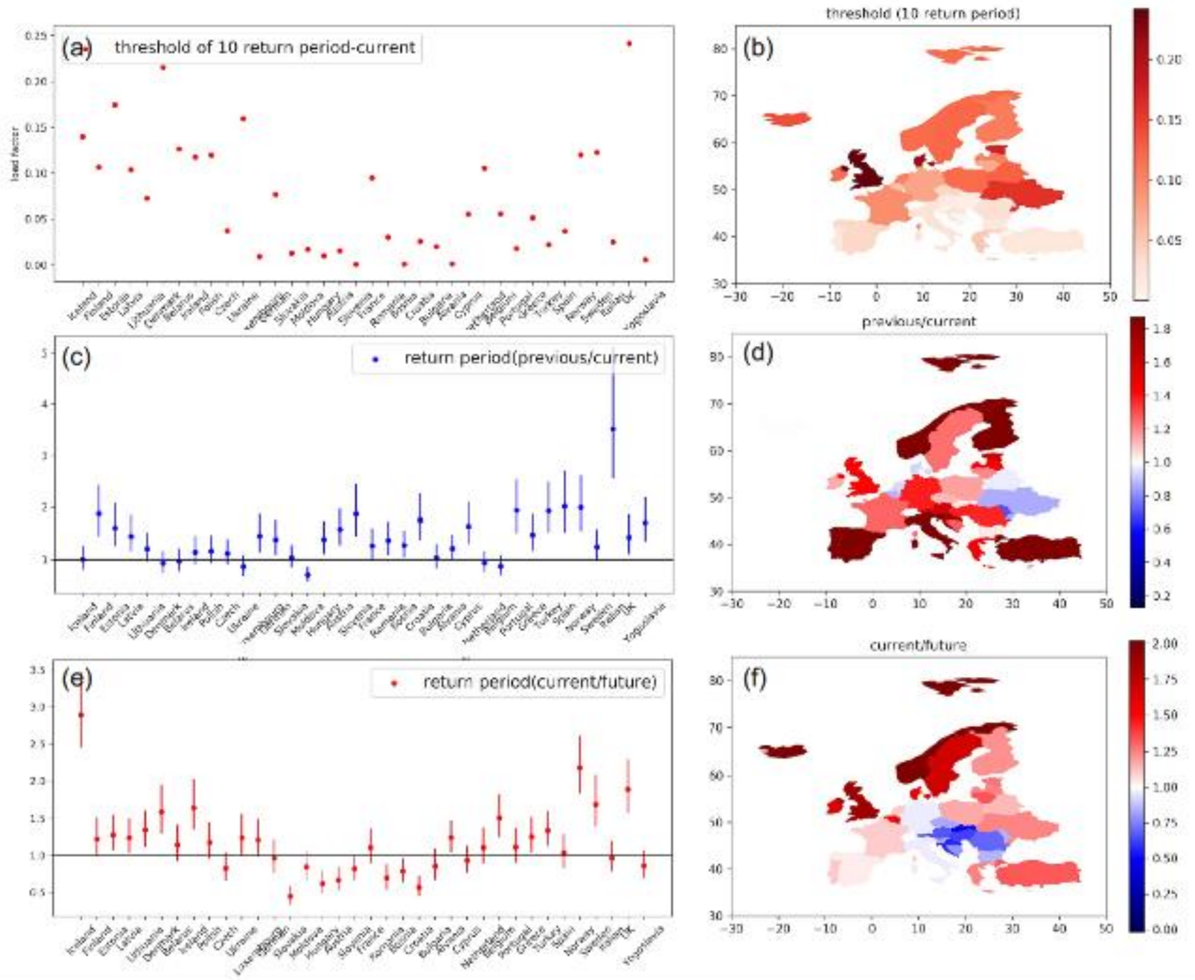

Fig.3.3. Boxplot and geographical distribution of (a,b) the return values corresponding to the 10-years events during 2000 to 2029 in each countries, which were referred as threshold; (c,d) the risk ratios between 1971-2000 and 2000-2029, and (e,f) the risk ratios between 2000-2029 and 2041-2069. The probability of low wind energy winter was increased when risk ratios were larger than 1. For boxplot (c,e), the red dot shows the median of all the grids in this region; the vertical bar shows the small uncertainty interval of the median. The 5% and 95% of the medians show the uncertainty interval.

In summary, most countries are experiencing more frequent low wind energy events compared with the past. In the future, low wind energy events will become more common in most countries, especially in northern countries where low wind energy winter will occur more frequently. Results can be used to determine the probability of future energy revenue deficits in long periods such as a full winter season for a large-scale producer. However, data and methods used bear several limitations. The lack of available observations of load factor or even wind at hub height is a limiting factor, as the models can hardly be verified for winds at such altitude. In addition, a larger model ensemble dataset would be essential to increase the robustness of the risk ratio distribution in the further research. This will be made possible through recent progress from the C3S in providing more simulations (currently about 50 simulations are available at a 3-hourly time step. In addition, the impact of high resolution remains to be determined.

References

DNV, G. (2018). Energy Transition Outlook 2018: A global, regional forecast of the energy transition to 2050. Last accessed Dec, 17, 2018.

Hersbach, H., Bell, B., Berrisford, P., Hirahara, S., Horányi, A., Muñoz-Sabater, J., ... & Thépaut, J. N. (2020). The ERA5 global reanalysis, QJ Roy. Meteor. Soc., 146, 1999–2049.

Jacob, D., Petersen, J., Eggert, B., Alias, A., Christensen, O. B., Bouwer, L. M., ... & Yiou, P. (2014). EURO-CORDEX: new high-resolution climate change projections for European impact research. Regional environmental change, 14(2), 563-578.

Philip, S., Kew, S., van Oldenborgh, G. J., Otto, F., Vautard, R., van der Wiel, K., ... & van Aalst, M. (2020). A protocol for probabilistic extreme event attribution analyses. Advances in Statistical Climatology, Meteorology and Oceanography, 6(2), 177-203.

3.3 Case #3: Wind energy drought under cold conditions.

3.3.1 Practical question posed by stakeholders

Space heating energy consumption in urban residential areas of the hot summer and cold winter zones in most of the northern hemisphere has increased dramatically during the last decade (Hu et al., 2016). The bulk coal combustion for heating was considered as one of the most important sources of air pollution (Li et al., 2017). For example, the air pollution in Northern China shows obvious seasonal characteristics, which was presented close relationship with massive space-heating in winter. Among renewable energy sources, wind energy is one of the most significant and potentially useful energy sources, which was expected to mitigate the fossil energy pollution in winter. Thus, it is crucial to consider the changes in renewables and in particular wind energy under cold conditions in Europe. Two questions will be asked. Are there significant differences in wind energy drought under different temperature conditions? Will wind energy drought risk be worse in cold conditions? The results contribute to optimize the transmission network and project the wind energy drought under different temperature conditions.

3.3.2 General strategy used to solve the question

Classical methods defined an extreme event as an exceedance of a threshold in the tail of the distribution of an event indicator. The definitions of extreme temperature threshold are often described by different standards, without a universal definition. Comparing the results based on different definitions helps to increase the robustness of the conclusion. In this case, three approaches were used to calculate the wind energy indicator. For experiment 1, for each winter, we calculated the moving average of the monthly mean temperature (window=31) and chose the 31 days with the minimum (maximum) value as the cold (warm) days; the indicator was the mean value of load factor during the cold (warm) days. For experiment 2, the threshold for extremely cold (warm) days was defined for the 10th (90th) percentile of regional mean temperature based on all the winter records during the 1979-2005; the indicator was the mean value of load factor during the cold (warm) days. For experiment3, the definition of cold (warm) days is the same as that in method 1; The indicator was the min value of load factor during the cold (warm) days.

3.3.3 Data and Method

As for Cases #1 and #2 we use Euro-CORDEX simulations. The research area and the 10 high-resolution climate projections from the Euro-CORDEX ensemble was selected as in case 2 (section 3.2.3). The 2m temperature and 100m wind speed were used in this study. The risk ratio was calculated as that in case 2. We also use the attribution framework as previously.

3.3.4 Results and discussion

We used each model ensemble separately to estimate the risk of load factor lower than the threshold under different temperature conditions. For all the experiments, in the EURO-CORDEX ensemble, the thresholds of ~10 years events of load factor in cold days are lower than that in warm days (Fig.3.1b). It implies that the intensity of wind energy droughts is more severe under cold conditions, which will certainly magnify the problem of energy shortage in cold winter. For all the experiments, under cold conditions, compared with the previous climate (1971-2000), the reduction of wind energy was significant in the current (2001-2029), and the risk ratios are larger than that in warm conditions based on all the experiments. In experiment 1, for example, for cold days, load factor lower than threshold becomes more than 2.26 times more probable in the current climate than in the 1971-2000 climate [risk ratio = (1.69,3.09)]. For that in warm days, there is a nonsignificant increase in frequency of wind drought in the current climate [risk ratio = (0.92,1.56)]. In the future, for experiment1, the probability of compound events with cold and lack of wind show significant increase and the risk of extreme events will be more than 1.6 times as probable than in the current climate. For warm days, the probability of extreme events is also systematically higher than that of current climate conditions, about 1.2 times. However, for experiment 2 and 3, in the future climate, the risk ratio under warm conditions is larger than that in cold conditions.

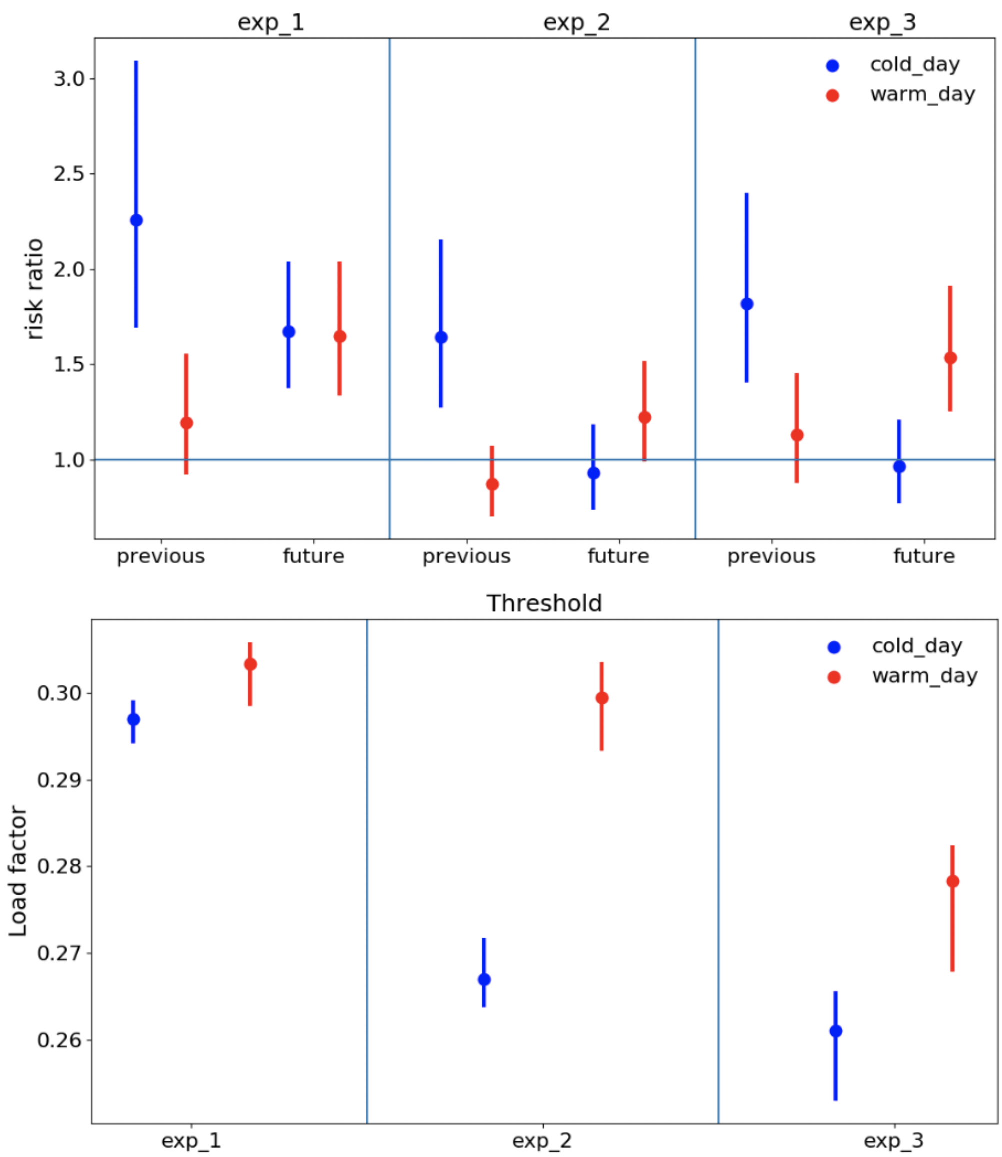

Fig.3.4. The (a) risk ratio and (b) threshold based on three different experiments. When the risk ratio <1, the low wind energy event is more frequent in the earlier climate period. The threshold is the return value of indicator of 10-years events during the current climate. The previous is from 1971 to 2000, the current climate is from 2000 to 2029, and the future climate is from 2041 to 2069.

In summary, for the whole of Europe, wind droughts are more intense and frequent in cold conditions, compared with that in warm conditions, magnifying the energy shortages in cold winters. In the future climate, the probability of compound events with cold and lack of wind shows unstable variations under different experiments. Considering more model simulations helps increase the robustness of the results. The result can be used to assess the wind energy shortage in cold winter and optimize the transmission network.

This case was taken as an example, but results should be considered as preliminary, and may not apply to subregions of the European continent. Given the uncertainty that can be seen in Fig.3.4 (top panel) on risk ratios, alternative statistical methods and indices should be considered also to strengthen the results robustness. For this, ensemble model simulation averaging with observational constraint as developed in WP2 should be considered. This should give a larger weight on more skillful simulations and thus a more reliable result. Differential trends in cold and warm conditions should be better understood by considering conditional attribution (e.g., with circulation analogs).

References

Hu, S., Yan, D., Cui, Y., & Guo, S. (2016). Urban residential heating in hot summer and cold winter zones of China—Status, modeling, and scenarios to 2030. Energy Policy, 92, 158-170.

Li, J., Lv, Q., Zhang, M., Wang, T., Kawamoto, K., Chen, S., & Zhang, B. (2017). Effects of atmospheric dynamics and aerosols on the fraction of supercooled water clouds. Atmospheric Chemistry and Physics, 17(3), 1847-1863.

3.4 Case #4: Improved wind power assessment for high-resolution climate models in complex terrain (Southern France).

3.4.1 Practical question posed by stakeholders

Renewable energy sources are gaining popularity among energy production authorities, countries, and energy companies due to their natural, low-cost, and environmentally friendly nature (Jung et al., 2014). Wind energy is one of the most significant and potentially useful energy sources. However, the use of wind energy has challenges. The initial investment costs are high, in particular. In addition, since wind turbines are not easily transportable, the wind energy potential of promising locations should be thoroughly investigated. Thus, for the wind energy producer, finding wind-rich locations to build wind farms is a critical issue.

Changes of wind energy should be anticipated at local scale, but models are currently too coarse to capture local effects. Wind energy assessment using low-resolution models might smooth out extreme-value signals in particular. Therefore, a high-resolution model is crucial for finding wind energy rich locations and site selection for wind farms. In addition, in some conditions such as anticyclonic conditions, winds may be lacking at large scale. In such cases the vertical wind distribution and flows in complex terrains (e.g., coastal and valley breezes) may be important energy sources. These, together with their trends, can hardly be assessed using current climate models due to a too coarse resolution.

The EUCP-WP3 explored the high-resolution models with the resolution of 3km. In this case, which needs to be much more developed in the future, we compared the simulation results of wind energy based on different resolution models, and analyzed the improvement of high-resolution models in wind energy assessment.

3.4.2 General strategy used to solve the question

In this case, we compared the wind speed evaluation results of the high-resolution model and the low-resolution models. The distribution of wind speed at hub height, together with its variability in space and time, is key for comprehensive wind resource assessment. Hub height (h_{hub}) of large wind turbines is typically about 100m. Thus, accurate datasets of wind speed at a hub-height of, e.g., 100m (w100) are necessary for the accurate assessment of wind energy resources. Firstly, we use machine learning algorithm to generate w100 output of high- and low-resolution models. Secondly, the spatial and temporal differences of w100 simulations based on different resolution models are compared.

3.4.3 Data and Method

The area selected for this study comprised most of the land in Southeast France, bounded by -4°W, 7.5°S and 43.5°W, 45.5°N, which is a complex-terrain area with effects of mountain slopes and coastal breezes. The high-resolution model datasets were calculated as the historical run forced by IPSL-CM5A-MR (1996-2005). It is the inner domain at 3km-resolution and the time resolution is 1 hour; The low-resolution model dataset is the EURO-CORDEX domain at 15km-resolution and the time resolution is 1 hour. The datasets in 2004 were analyzed in this research, both spatial and temporal distribution was considered. The meteorological factors, including surface wind, w100, 2m temperature (tas), and temperature in 850hPa (ta850) were used.

3.4.4 Results and discussion

Fig.3.5 shows the regional mean w100 based on high- and low- resolution climate models in 2004. The dataset in 17-Dec-2004 was also selected to compare the wind speed distribution on a daily scale. For the two models, regions with high wind speeds are generally uniform in space. The regional mean of w100 in the high-resolution model is slightly larger than that in low-resolution model. This is partly because the extreme records are smoothed out in the low-resolution data set. In addition, the high-resolution models are helpful to find areas with higher wind speeds. For example, in the northeastern region of the research area, there is no obvious wind speed signal in the low-resolution model, but in the high-resolution model, wind-rich areas are identified, which is meaningful to find wind energy rich locations and build wind farms. For the seasonal cycle, in all the months, wind speed from high-resolution models is higher than that in low-resolution models, approximately. Especially in winter with high wind speed, high resolution models show unique advantages over the high wind speed identification. The wind speed values of the high-resolution models are systematically higher than those of the low-resolution model, which is consistent with the results of the spatial analysis.

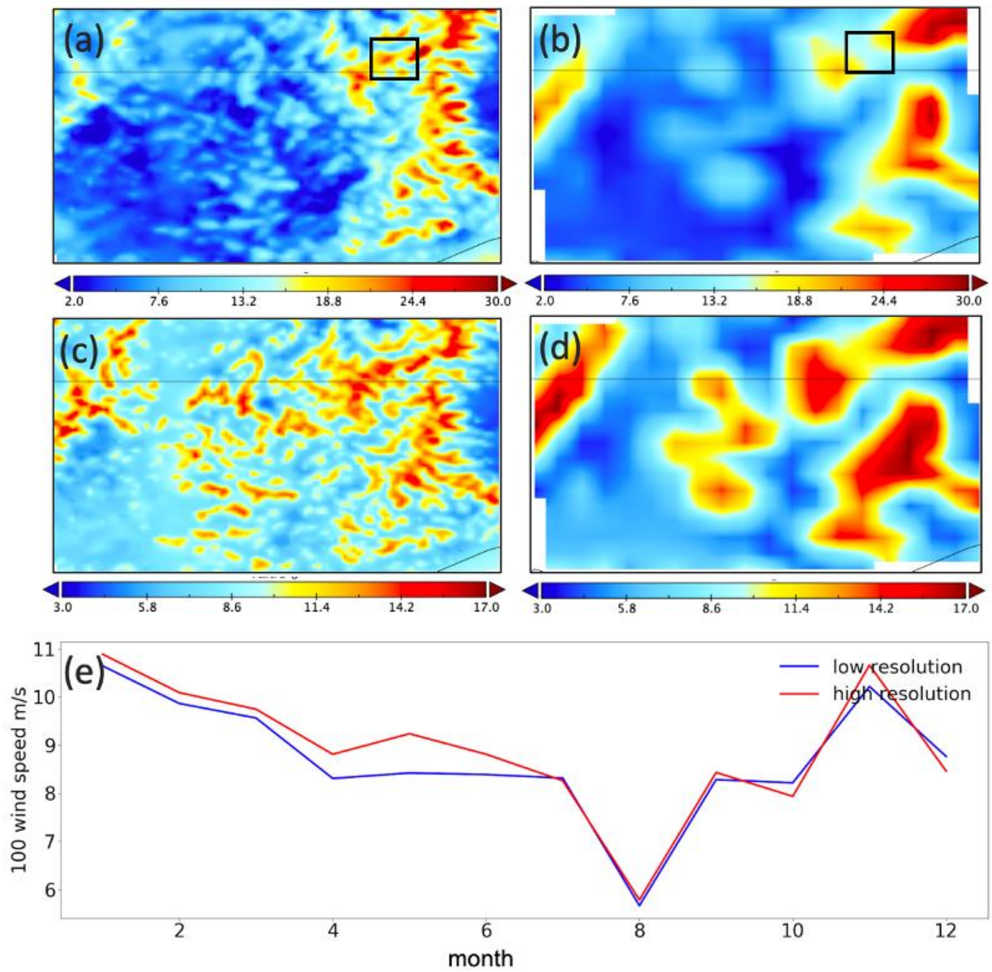

Fig.3.5. Geographical distribution of the (a-b) annual mean value of wind speed in 2004 and the (c-d) daily mean value of wind speed in 17-Dec-2004. The left figures show the wind speed from the high-resolution model and the right figures show that from the low-resolution model. (e) Compared the seasonal cycle of w100 based on two different models.

Capturing the correct wind variability at local, near site scale is a big challenge for using wind energy. High resolution model is essential for the wind assessment and the identification of wind-riches location. The result in this research shows the model resolution affects the wind energy assessment and the high-resolution model shows unique advantages for the high wind speed identification. However, high-resolution climate models are not long enough (1996-2005) for the extreme statistics currently, which challenges the projection research at a wind farm site. Thus, it is crucial to explore long-term high-resolution climate simulations in the further research.

This case is clearly for future exploration, and our results are extremely preliminary. Investigation of extreme wind calms should in particular be carried out, using several such models. More models should be considered to address structural uncertainty. High resolution really opens the door to improved wind energy assessments, but this remains to be fully demonstrated.

References

Jung J, Broadwater R P. Current status and future advances for wind speed and power forecasting. Renewable and Sustainable Energy Reviews, 2014, 31: 762-777.

3.5 Case #5: Wind drought in Eastern USA.

3.5.1 Practical question posed by stakeholders

To achieve climate neutrality, a vast effort to decarbonize the energy sector is taking place in many countries worldwide, defining green transition frameworks. One of the pillars of this framework is the massive development of renewable energy, especially wind and solar. This is an opportunity to stimulate the economy, promote green jobs, enhance competitiveness, address energy poverty and reduce energy dependence (nowadays, Europe is heavily dependent on foreign oil and gas sources), among others (IEA, 2021).

However, wind farm owners, operators, and project developers face the challenge of understanding wind variability at several time scales to run their business successfully. Within a context of a higher share of renewables in the electricity mix, transmission system operators will also need to understand climate variability that impacts electricity generation to guarantee energy supply and dimension transmission and backup facilities. On top of that, the risks of extreme events affect all these decisions.

One of these events happened in 2015 in the United States, during the first quarter of 2015 (January–March), surface wind speeds were below normal conditions (Lledó et al, 2017), and some companies experienced financial problems due to the lack of energy production and revenues (Meyer, 2015). Nowadays, in the United States, 5% of the total electricity demand is covered by wind power. This percentage is expected to increase in the forthcoming years significantly according to the green transition frameworks mentioned before.

3.5.2 General strategy used to solve the question

While the energy sector has routinely been using weather forecasts of up to 15 days (Dubus, 2010), beyond this time horizon, climatological data (typically 30-year averages) are used. A common assumption in this method is that future conditions will be similar to past conditions. This assumption entails one major shortcoming, climatology cannot predict events which have never happened before, which can be particularly harmful and whose prediction is of special interest for stakeholders. Our knowledge of climatology is based on a finite sample of past events. This sample is limited in time, and doesn't need to be fully representative of what can happen. Moreover, a climatological approach does not take into account changes in atmospheric dynamics, such as those caused by climate change. Climate change may render past conditions useless for predicting future events, as they may no longer be reproduced.

Decadal climate predictions have witnessed considerable improvements in the last decade demonstrating that probabilistic forecasting can inform better decision making at some temporal scales and regions. However, despite this improvement, climate predictions come with a new set of challenges for users: information is often un-tailored and hard to understand or apply in a decision-making context. Further research is needed to broaden our knowledge of the predictability and usability of climate predictions and the requirements of energy companies and transmission system operators.

3.5.3 EUCP data and methods used in the case study, including EUCP specific advances

We used available decadal predictions of sub-daily surface wind speed in this case study. The Decadal prediction systems employed contribute to the Decadal Climate Prediction Project (DCPP; Boer et al., 2016) of the Coupled Model Intercomparison Project Phase 6 (CMIP6; Eyring et al., 2016). These include 45 ensemble members from 5 forecast systems (Table 3.2). The ECMWF Reanalysis v5 (ERA5; Hersbach et al., 2020) has been used as a reference dataset to perform the forecasts quality assessment.

Table 3.2. Forecast systems that provide sub-daily surface wind speed data contributing to the CMIP6/DCPP and their specifications (available simulations at the time of the study).

Forecast system	nº of DCPP members	Near-real time data	Spatial resolution	Month of initialisation	Reference
EC-Earth3-i1	10	No	0.7º x 0.7º	November	Bilbao et al. (2021)
EC-Earth3-i2	5	No	0.7º x 0.7º	November	Tian et al. (2021)
EC-Earth3-i4	10	Yes	0.7º x 0.7º	November	Bilbao et al. (2021)
IPSL-CM6A-LR	10	No	1.25º x 2.5º	January	Boucher et al. (2020)
MPI-ESM1.2-HR	10	No	0.9º x 0.9º	November	Müller et al. (2018)

The multi-model ensemble has been built by pooling all members together to compute the ensemble mean (for the deterministic forecasts) and probabilities for each tercile category (for the probabilistic forecasts). The predictions for the average of years 1-5 have been evaluated over the 1961-2021 period (start dates 1960-2016). The Anomaly Correlation Coefficient (ACC; Wilks, 2011) and Root Mean Squared Error Skill Score (RMSSS; Wilks, 2011) have been used to estimate the quality of the deterministic products. For the probabilistic products based on tercile and quintile categories, the Ranked Probability Skill Score (RPSS; Wilks, 2011) and Relative Operating Characteristic Skill Score (ROCSS; Kharin and Zwiers, 2003) have been used. A two-sided t-test has been applied to estimate the ACC significance at the 95% confidence level accounting for the time series' autocorrelation (Von Storch and Zwiers, 2001). The Random Walk test (DelSole and Tippett, 2016) has been used to assess the significance of the skill scores at the 95% confidence level.

3.5.4 Results and discussion

The multi-model forecast shows skill in predicting the surface wind speed variations over some areas of the considered region according to ACC and ROCSS (for below normal and above normal categories) statistics, especially over the eastern part of the USA (Fig.3.6). Instead, the RMSSS and RPSS show mostly negative values, meaning that the climatological forecast performs better than the multi-model ensemble.

However, the multi-model could not be used for potential operational forecast generation since only the predictions of one of the forecast systems are issued in real-time (EC-Earth3-i4; see Table 2). In order to assess the quality of these operational real-time predictions, the EC-Earth3-i4 skill has been computed and is shown in Fig.3.7, which presents a similar skill pattern for the surface wind speed predictions. Note that the EC-Earth3 forecasts are provided in a higher spatial resolution than the multi-model forecasts (as the simulations should be interpolated to the coarsest grid among the models for the later).

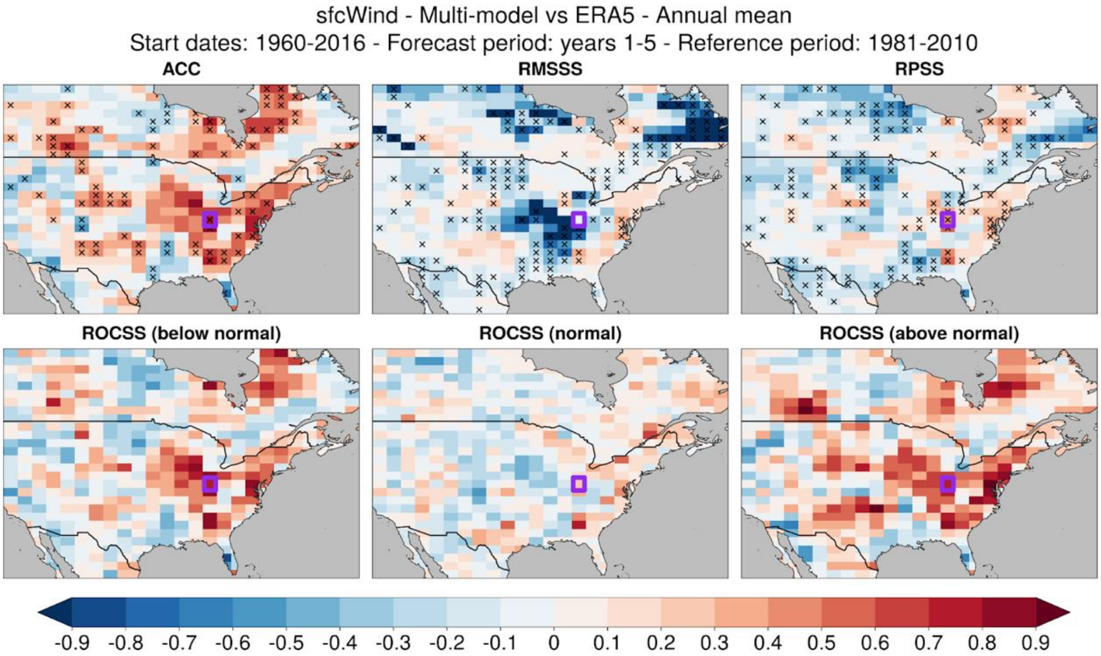

Fig.3.6. Multi-model skill in predicting the surface wind speed for the forecast years 1-5.

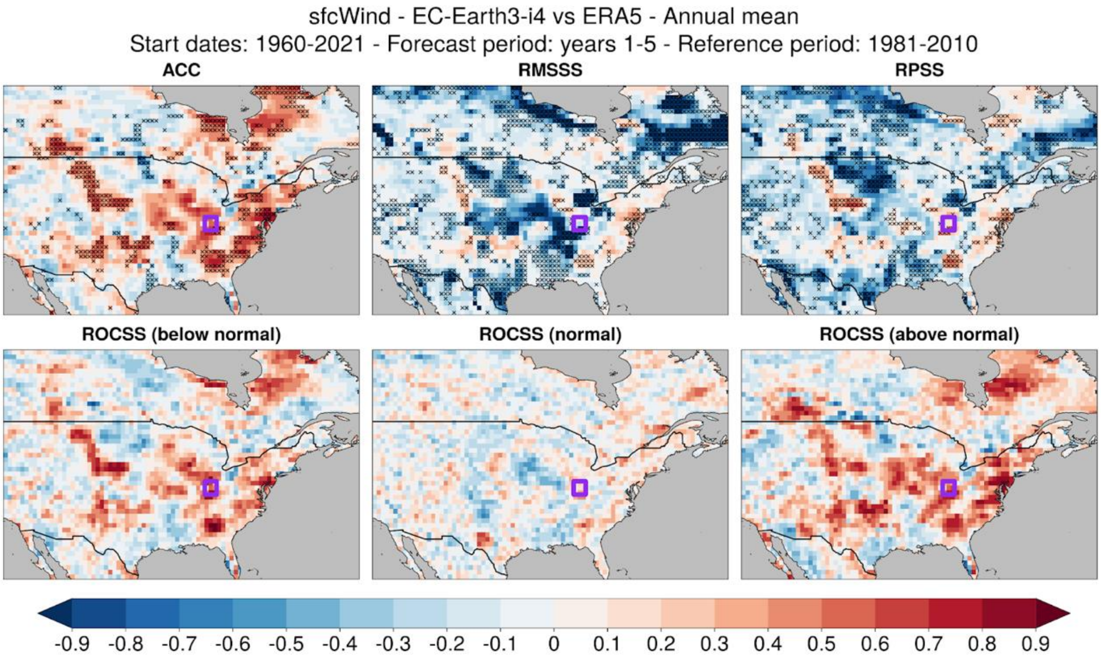

Fig.3.7. EC-Earth3-i4 skill in predicting the surface wind speed for the forecast years 1-5.

To illustrate the potential application of decadal predictions for wind energy, a specific location has been selected: 39ºN, -85ºE (Fig.3.8). The probabilities of each tercile category are shown with colours, while the observed categories are shown with dots for each time step (5-year averages). Besides, the ROCSS is provided together with the forecast, which shows positive values for all the categories meaning that the EC-Earth3-i4 forecasts are more skillful than climatology in this location. Apart from the hindcast period (for which observations are also shown), the actual forecast for the next years is also provided. For instance, the last time step corresponds to the predictions for 2022-2026 created with the start date 2021, which indicates below-normal conditions for the surface wind speed over the considered location.

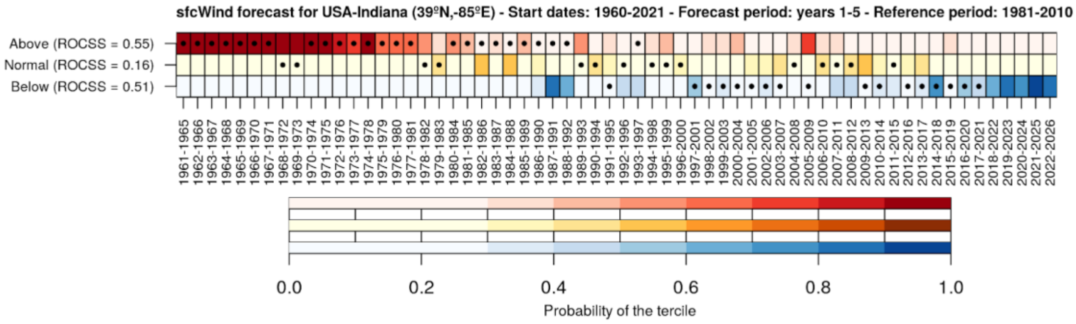

Fig.3.8. EC-Earth3-i4 forecast of the surface wind speed for the forecast years 1-5 over Indiana, USA.

The main difficulties of this study have been the huge amount of data (subdaily data from multiple forecast systems over more than 60 years), the short ensemble size for forecast generation (as only a few systems provide subdaily wind data and only one of them is operational), and how to adapt and communicate the probabilistic information to users (in addition to the interpretation of the skill estimates).

As potential improvements of the study, it could be considered touse hybrid statistical-dynamical techniques to try to improve the skill of the dynamical models. Besides, the increase of the ensemble size as well as the increase of themodels' spatial resolution could improve the forecast quality.

References

Bilbao, R., Wild, S., Ortega, P., Acosta-Navarro, J., Arsouze, T., Bretonnière, P.-A., Caron, L.-P., Castrillo, M., Cruz-García, R., Cvijanovic, I., Doblas-Reyes, F. J., Donat, M., Dutra, E., Echevarría, P., Ho, A.-C., Loosveldt-Tomas, S., Moreno-Chamarro, E., Pérez-Zanon, N., Ramos, A., Ruprich-Robert, Y., Sicardi, V., Tourigny, E., and Vegas-Regidor, J. (2021). Assessment of a full-field initialized decadal climate prediction system with the CMIP6 version of EC-Earth, Earth Syst. Dynam., 12, 173–196, https://doi.org/10.5194/esd-12-173-2021

Boer, G. J., Smith, D. M., Cassou, C., Doblas-Reyes, F., Danabasoglu, G., Kirtman, B., Kushnir, Y., Kimoto, M., Meehl, G. A., Msadek, R., Mueller, W. A., Taylor, K. E., Zwiers, F., Rixen, M., Ruprich-Robert, Y., and Eade, R. (2016). The Decadal Climate Prediction Project (DCPP) contribution to CMIP6, Geosci. Model Dev., 9, 3751–3777, https://doi.org/10.5194/gmd-9-3751-2016

Boucher, O., Servonnat, J., Albright, A. L., Aumont, O., Balkanski, Y., & Bastrikov, V., et al. (2020). Presentation and evaluation of the IPSL-CM6A-LR climate model. Journal of Advances in Modeling Earth Systems, 12, e2019MS002010. https://doi.org/10.1029/2019MS002010

DelSole, T., & Tippett, M. K. (2016). Forecast Comparison Based on Random Walks, Monthly Weather Review, 144(2), 615-626. https://doi.org/10.1175/MWR-D-15-0218.1

Dubus, L. (2010). Practises, needs and impediments in the use of weather/climate information in the electricity sector, in Management of Weather and Climate Risk for the Energy Sector, A. Troccoli, ed., NATO Science Series, Springer Academic Publisher, ISBN 97890-481-3691-9.

Eyring, V., Bony, S., Meehl, G. A., Senior, C. A., Stevens, B., Stouffer, R. J., and Taylor, K. E. (2016). Overview of the Coupled Model Intercomparison Project Phase 6 (CMIP6) experimental design and organization, Geosci. Model Dev., 9, 1937–1958, https://doi.org/10.5194/gmd-9-1937-2016

Hersbach, H, Bell, B, Berrisford, P, et al. The ERA5 global reanalysis. Q J R Meteorol Soc. 2020; 146: 1999– 2049. https://doi.org/10.1002/qj.3803

International Energy Agency (2021). Spain 2021, Energy Policy Review. Country report. May 2021. Retrieved from https://www.iea.org/reports/spain-2021

Kharin, V. V., & Zwiers, F. W. (2003). On the ROC Score of Probability Forecasts, Journal of Climate, 16(24), 4145-4150. https://doi.org/10.1175/1520-0442(2003)016%3C4145:OTRSOP%3E2.0.CO;2

Lledó, L., Bellprat, O., Doblas-Reyes, F. J., & Soret, A. (2018). Investigating the effects of Pacific sea surface temperatures on the wind drought of 2015 over the United States. Journal of Geophysical Research: Atmospheres, 123, 4837– 4849. https://doi.org/10.1029/2017JD028019

Meyer, G. (2015). US clean energy suffers from lack of wind, Financial Times. 1 September 2015. Retrieved from https://www.ft.com/content/b967b6d4-5058-11e5-8642-453585f2cfcd

Müller, W. A., Jungclaus, J. H., Mauritsen, T., Baehr, J., Bittner, M., Budich, R., et al. (2018). A higher-resolution version of the Max Planck Institute Earth System Model (MPI-ESM1.2-HR). Journal of Advances in Modeling Earth Systems, 10, 1383– 1413. https://doi.org/10.1029/2017MS001217

Kharin, V. V. and Zwiers, F. W. (2003). On the ROC Score of Probability Forecast. Journal of Climate. https://doi.org/10.1175/1520-0442(2003)016%3C4145:OTRSOP%3E2.0.CO;2

Tian, T., Yang, S., Karami, M. P., Massonnet, F., Kruschke, T., and Koenigk, T. (2021). Benefits of sea ice initialization for the interannual-to-decadal climate prediction skill in the Arctic in EC-Earth3, Geosci. Model Dev., 14, 4283–4305, https://doi.org/10.5194/gmd-14-4283-2021

Von Storch, H. and Zwiers, F. W. (2001). Statistical Analysis in Climate Research. Cambridge: Cambridge University Press. https://doi.org/10.1017/CBO9780511612336

3.6 Case #6: Pluvial flood hazard and risk in Milan.

3.6.1 Practical question posed by stakeholders

Flood risk is accountable for the largest economic losses in Europe and in Italy, and is responsible for damage exceeding 158 and 38 billion Euros respectively over the period 1980-2020 (Mysiak et al., 2022). Whereas floods caused by high river stages and storm surges have been addressed via the hazard mapping and assessment mandated by the Floods Directive (2007/60/EC), the hazard arising from spontaneous overland runoff from extreme precipitation events in urban context received lower attention. The projected climate change in Europe is expected to increase the intensity and frequency of extreme rainfalls, which in combination with the continuing land conversion and urban expansion will lead to higher pluvial flood risks and expected damage and loss. It is important therefore to design adequate financial protection and risk mitigation strategies such as sustainable urban drainage (SUDS). We have explored in this case the pluvial hazard risk and risk-mitigation measures over the city of Milan in northern Italy.

3.6.2 General strategy used to solve the question

Here we use a simplified and computationally efficient raster-based model based on a hierarchical filling and spilling algorithm. The same model has been used for the Copernicus Sectoral Information System (C3S) for pluvial flood risk assessment in 20 European cities, forced by dynamically downscaled climate reanalysis (Essenfelder et al., 2021). Building upon that work, we extended the analysis using the convection-permitting climate simulations produced in EUCP (WP3) and simulated the effects of the nature-based solutions, reducing the pluvial hazards and risk. Green Infrastructures (GI) (EEA, 2017) are defined as a strategically planned network of green and natural elements supporting a wide range of services and benefits to people (EC, 2013a). In urban environments, GI can be open green spaces, as parks and gardens, green roofs, green alleys, permeable pavements and vegetated buffers. These elements contribute to flood regulation increasing the soil capacity to retain and infiltrate water controlling the storm-water runoff and peak flow (EC, 2013b). To increase and maximise the flood regulation capacity of GI, they should be strategically distributed and connected across the city. Connectivity is considered a key pillar to maintain healthy and well-functioning ecosystems that can support ecological functions and delivery of services (Mitchell et al., 2013, 2015).

3.6.3 EUCP data and methods used in the case study, including EUCP specific advances

Data and methods are developed in depth in Deliverable 4.3 to which the reader is referred to for more details. For climate forcing, they use high resolution, convection-permitting climate simulations produced in WP3 over the ALP-3 domain, with Generalised Extreme Value (GEV) distributions to estimate maximum rainfall rates for probabilities ranging from 0.5 (return period RP 2 years) to 0.001 (RP 1000 years). Pluvial flood hazard maps were generated for each rainfall probability using a simplified raster-based model based on a hierarchical filling and spilling algorithm (Samela et al., 2020). Direct tangible damages to urban buildings were estimated using stage-damage models (Huizinga et al., 2017) and reconstruction costs were used for economic impact. Then for adaptation, the existing green infrastructure (GI) network was extracted from the European Settlement Map of 2017, reclassified to 100m grid (Ferri et al., 2017), and we identified areas that simultaneously contribute to improving the connectivity of the GI network as well help to reduce the pluvial flood hazard. We then built 3 scenarios of green infrastructure's improvement and ran a pluvial hazard model for each scenario for extreme events.

3.6.4 Results and discussion

Models predict an increase in the intensity of extreme hourly rainfall rates throughout the 21st century. A 1-in-5 years event is expected to increase by 2.2% and 14.2% by the mid-century and late-century, respectively, while a 1-in-100 years event is expected to increase in intensity by 44.0% and 209.1%, respectively. The estimated expected annual damage (EAD) under the historical climate period for Milan is 744 million EUR, with the historical city centre (including train station area) being one of the most affected areas. As shown in Fig 3.9, the EAD from direct tangible damages are expected to increase by 1.36% (10.1 million EUR) and 9.49% (70.6 million EUR) by mid- and late-century, respectively. Regarding adaptation, the scenarios were examined and identified a number of city areas with potential to reduce flood damages. The Green City scenario offers options to develop greener areas, including rooftops. These were shown to reduce flood risk.

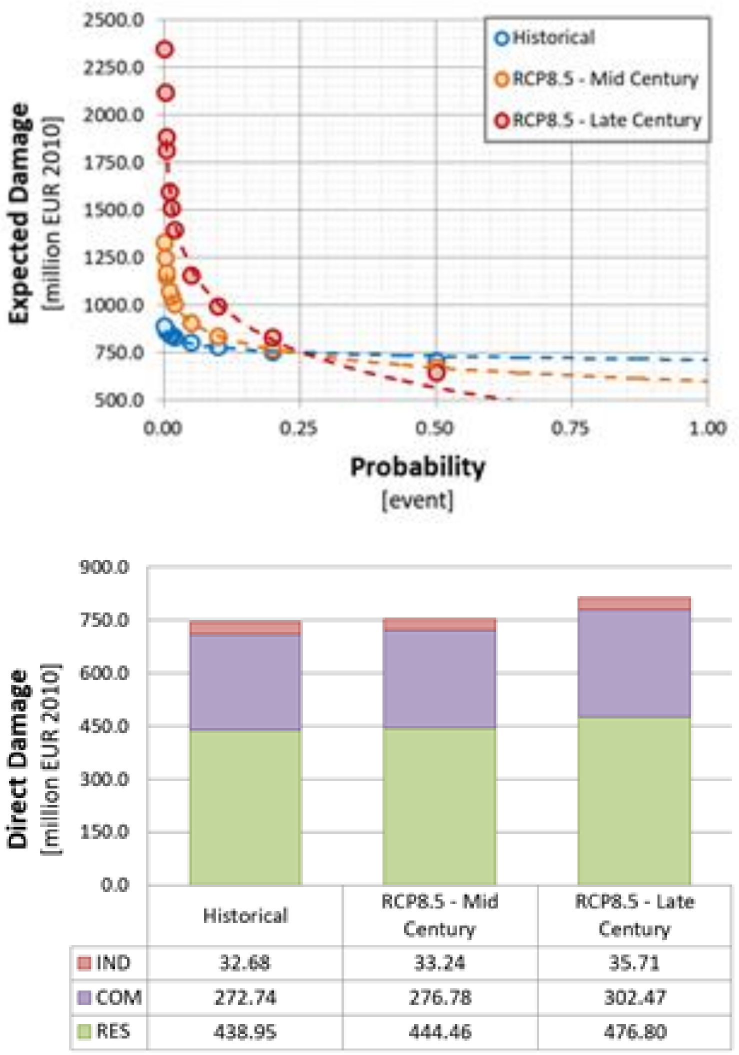

Fig.3.9. Expected direct tangible damages due to pluvial flooding in Milan under the historical, RCP 8.5 mid-century, and RCP 8.5 late-century climate scenarios. On the left, the expected damage – probability curve. On the right, the expected annual damage (EAD) for each climate scenario.

Nature-based solutions (NbS) can provide means to mitigating climate risks - in this case through water flow regulation. For many stakeholders, the performance of NbS under extreme hazard conditions and their integrity in the face of climate change remains unclear. In this work, we have demonstrated the usefulness of the EUCP convection-permitting climate simulations for the urban climate risk assessment and adaptation planning. This works builds upon and extends the C3S Pluvial Flood Risk Assessment in Urban Areas developed by CMCC and other partners. By using the EUCP climate simulation, we improved the existing pluvial hazard and risk assessment and demonstrated how NbS can mitigate the risk, while producing additional benefits in terms of temperature regulation, air quality improvement (by removal particle pollution), and protect soil and biodiversity.

3.7 Case #7: Extreme sea levels along Upper Adriatic Sea coasts.

3.7.1 Practical question posed by stakeholders

Coastal hazards such as erosion, storm tide inundation and permanent flooding, can have strong adverse impacts on coastal regions, with loss of sandy shores, damage to settlements, infrastructure, heritage sites, ecosystems. Climate change can exacerbate these impacts due to rising sea levels and increasing impacts of waves and storms. Coastal areas along the Upper Adriatic Sea (Italy) are highly exposed and vulnerable to coastal floods and the flood risk is projected to further increase as a result of sea level rise (SLR) and local subsidence. We focus on two coastal cities - Rimini (~ 150,000 residents) and Cesenatico (~ 27,000 residents) in Emilia Romagna, both among the most important destinations of summer tourism. For both areas, the question is to assess the coastal flood risk under current and future scenarios and analyse the performance of implemented or planned/hypothetical coastal defence measures.

3.7.2 General strategy used to solve the question

We use a high-resolution hydrodynamic model to identify areas prone to coastal floods under the baseline (undefended) and the structural coastal protection (defended) scenario. The defended scenarios account for the effect of coastal barriers based on the design of *Parco del Mare*, an urban renovation project under construction in Rimini. The same defence structure is modelled along the coastal perimeter of Cesenatico. On the base of probabilistic hazard assessment we estimate the expected annual damage (EAD) using a locally-calibrated damage model. Well informed coastal risk mitigation and adaptation actions require accurate and detailed information about the characterisation of coastal flood hazard and the performance of coastal defence options. Cost-benefit analysis (CBA) is widely used to evaluate the economic desirability of a disaster risk reduction (DRR) project (Jonkman et al., 2004; Mechler, 2016; Price, 2018), helping decision-makers in evaluating the efficacy of different adaptation options (Bos and Zwaneveld, 2017; Kind, 2014).

3.7.3 EUCP data and methods used in the case study, including EUCP specific advances

We use a model of coastal inundation, representing the combined effects of high tide, storm surge and action of waves. The latter combines wave setup with wave periodicity of incoming breaking waves. Estimates of storm surge and tides and waves are obtained for the North Adriatic up to year 2100 by combining reference hazard scenarios derived from the analysis of historical records (Armaroli et al., 2012; Armaroli and Duo, 2018; Perini et al., 2017, 2016, 2011) with regionalised projections of SLR (Vousdoukas et al., 2017) and local vertical land movements (VLM) rates (Carbognin et al., 2009; Perini et al., 2017). We consider four scenarios of extreme sea level (ESL), ranging from low intensity-high frequency to high intensity-low frequency, under current and future (2050 and 2100) conditions. Then scenarios (defended and undefended) are compared.

3.7.4 Results and discussion

Extreme Sea Level (ESL) scenarios based on modeling have been translated into inundation scenarios and Expected Annual Damage (EAD). In Rimini, the EAD grows from around 650 thousand Eur under historical conditions to 2.8 million Eur in 2050 and more than 32.3 million Eur in 2100. Under more extreme ESL scenarios, the benefits of the Parco del Mare project protecting the southern part of Rimini become more evident, avoiding about 65% of the expected damages in the defended scenarios compared to the undefended ones. In Cesenatico, the average EAD for the undefended scenario grows from around 270 thousand Eur under historical conditions, to 1.7 million Eur in 2050 and almost 26 million Eur in 2100. In our simulations, the designed defence structure (a static barrier with height of 2.8 m along 7.8 km of coast) is able to avoid most of the damage inflicted to residential buildings. The measure becomes less efficient for the most extreme scenarios in 2050 and 2100, when the increase in TWL causes the surmounting of the barrier (Fig.3.10).

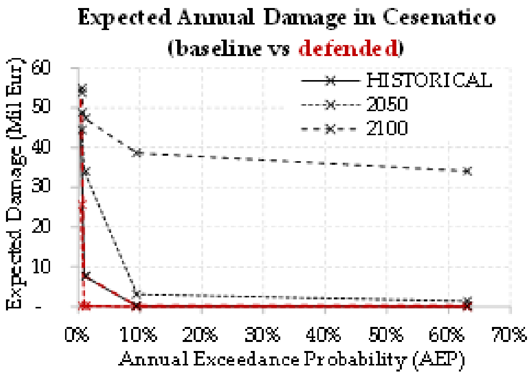

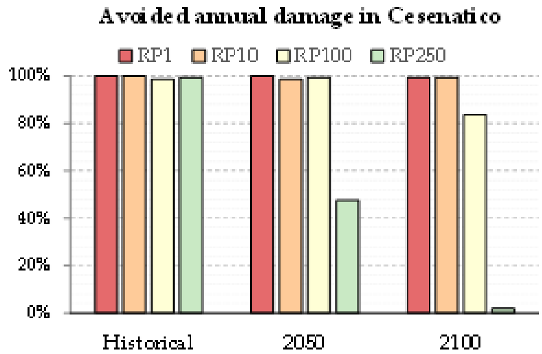

Fig.3.10. Cesenatico: Expected Annual Damage (EAD) according to undefended scenario up to 2100 [left]; EAD reduction thanks to hazard mitigation offered by the coastal barrier [right].

High performance computing and advances in numerical computing algorithms have made it possible to develop a new generation of hazard and risk models and high-resolution exposure mapping. We estimated a cost-benefit ratio of coastal defence measures, including through nature-based (or ecosystem services-related) solutions. We estimated an increase in expected damage for both urban areas from 2021 to 2100: in Cesenatico the EAD grows by a factor 96, in Rimini by a factor 49. Our results show that profitability of the coastal defence projects grow over time in both locations.

3.8 Case #8: Multi-year prediction of dry conditions over global wheat harvesting regions.

3.8.1 Practical question posed by stakeholders

Unfavorable and extreme climate events such as drought heavily impacts the agriculture sector and food security, and the impact of these climate hazards is expected to increase over the upcoming decades due to anthropogenic climate change. Recently developed decadal climate forecast systems aim to provide a future outlook of the Earth's climate system for a period ranging from 1 to 10 years. Skilful prediction of extreme climate events using this climate information shows potential for supporting risk reduction and adaptation strategies in the agriculture sector, fostering food security and better planning crop insurance schemes. In recent years, the stakeholder involved in this case study was actively involved in exploring the added value of decadal climate information for building a reliable climate service for agricultural needs on a multi-annual to decadal timescale. In this context, the stakeholder was interested in knowing the skill of decadal climate information in predicting drought conditions on a multi-annual timescale over the global wheat harvest areas.

3.8.2 General strategy used to solve the question

The general strategy is to study the evolution of multi-year summer drought conditions during the six months previous to the harvesting month (indicated with the color bar of the map in Fig.3.11a) using decadal climate predictions. The occurrence of drought conditions during the considered months at the corresponding wheat producing areas are evaluated using the user-relevant agro-climatic index: Standardized Precipitation Evapotranspiration Index (SPEI6). Following the index estimation, we assessed the skill of the climate model at predicting drought conditions for the forecast years 1 to 5 and developed a forecast product to share the forecast of drought conditions for the years 2020-2024 over global wheat harvesting regions with the stakeholder.

3.8.3 EUCP data and methods used in the case study, including EUCP specific advances

This case study uses decadal forecasts (42 members in total) produced by four European institutions which update their forecast annually: 10 members from EC-Earth3 (Bilbao et al., 2021); 10 members from DePreSys4 (Sellar et al., 2020), 16 members from MPI-ESM1-2-LR (Mauritsen et al., 2019) and 6 members from CMCC-CM2 (Cherchi et al. 2018). The ECMWF Reanalysis v5 (ERA5; Hersbach et al., 2020) has been used as a reference dataset to perform the forecasts quality assessment.

The drought conditions are estimated using SPEI6 index. SPEI6 is the standardized six-months accumulated climate water balance defined as the difference between monthly precipitation and potential evapotranspiration (PET). Such an index is chosen primarily due to it's widespread acceptance by the agricultural user community as a representative of drought conditions in recent years. The computed index is bias-adjusted using the calibration approach presented in Doblas-Reyes et al. (2005). After the calibration, we construct a large multi-model ensemble by pooling all the members of each individual forecast system together. The detailed methodology is presented in Solaraju-Murali et al., 2021. We use the ranked probability skill score (RPSS) as a measure of predictive skill, to assess the forecast quality of predicted probabilities of tercile categories by decadal forecasts. The climatological forecast is considered as a baseline while estimating the RPSS.

3.8.4 Results and discussion

Fig.3.11b presents the predicted likelihood map (in %) of the most likely tercile (labeled as below-normal, normal and above-normal) of drought occurrences using SPEI6 corresponding to the wheat harvesting season (in Fig. 3.11a). The probabilities of the most likely tercile category shows an increase in the dry conditions (below-normal category) over most of the wheat growing regions for the years 2020-2024.

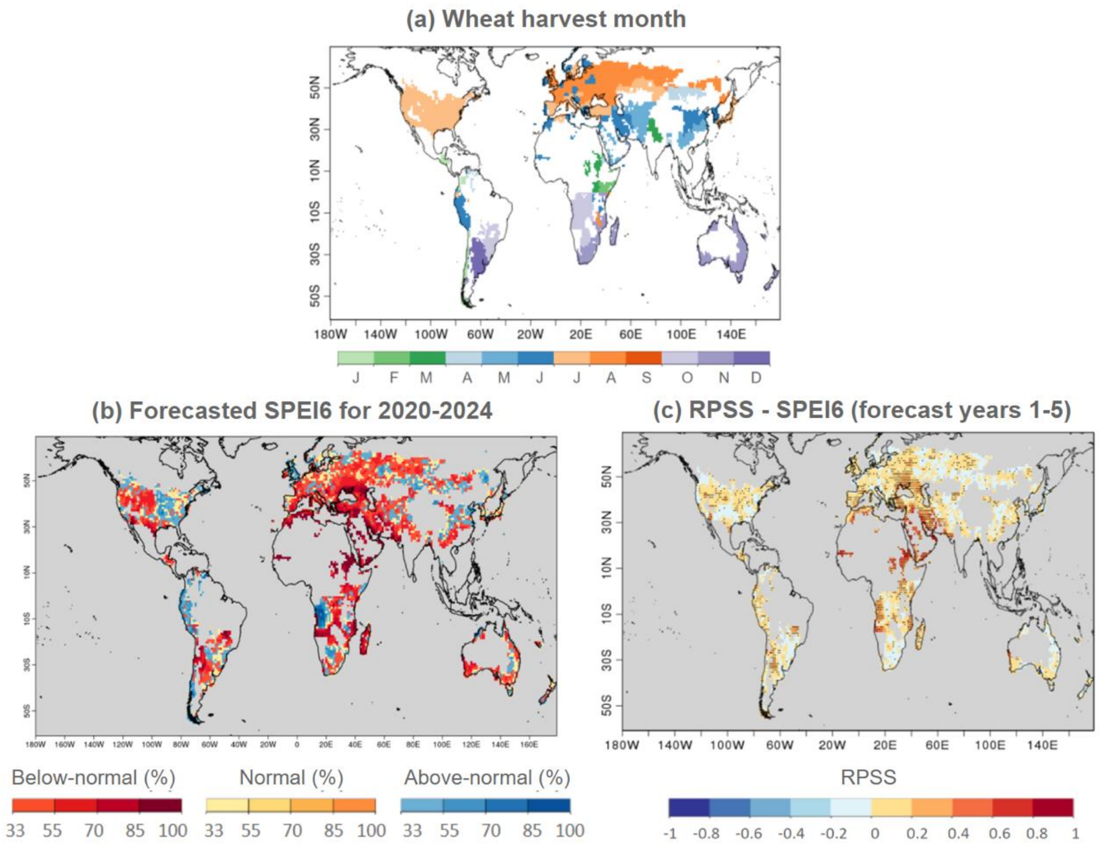

Fig.3.11. (a) Wheat harvest months that are used as a target month to study SPEI6. (b) Most likely tercile category (below-normal, normal and above-normal) of SPEI6 over the global wheat harvesting regions, in which the colored grids show the category with the highest probability of occurrence. (c) Ranked Probability Skill Score, RPSS of SPEI6 forecast averaged over years 1–5, during the wheat harvest month in each area, for the period 1961–2014.

In this study, the skill in predicting certain event categories (such as the ones presented in Fig. 3.11b) is investigated using the RPSS. The skill score is 1 for a perfect forecast and 0 for the forecasts that do not perform any better than the reference forecast, in our case a climatological forecast. Negative values indicate that the forecast system performs worse than the reference. A positive and significant value of RPSS is found over several regions, particularly over the Mediterranean, Middle East, and South Africa, whereas a negative skill is found over parts of the United States, South America, Russia and northern Australia. This indicates that the decadal predictions exhibit an added value with respect to a simple climatological multi-year approach in predicting drought conditions using SPEI6.

The proposed methodology in this assessment can be easily adapted to different crops (such as rice and maize) or to other sectors where water management plays a fundamental role. While we see encouraging results, this assessment has been carried-out with the available decadal forecast systems that are annually updated by European institutions for operational purposes. Due to this, the total number of ensemble members used for this analysis is limited. Several studies have pointed out the need for large ensembles to achieve more reliable and skillful forecasts (Scaife and Smith, 2018, Smith et al., 2019). To address this, constructing a much larger ensemble by using decadal prediction systems that contributed to CMIP6 needs to be explored in the future analysis.

References

Bilbao, R., Wild, S., Ortega, P., Acosta-Navarro, J., Arsouze, T., Bretonnière, P. A., et al (2021). Assessment of a full-field initialised decadal climate prediction system with the CMIP6 version of EC-Earth. Earth System Dynamics. https://doi.org/10.5194/esd-12-173-2021

Cherchi, A., Fogli, P. G., Lovato, T., Peano, D., Iovino, D., Gualdi, S., et al. (2018). Global Mean Climate and Main Patterns of Variability in the CMCC-CM2 Coupled Model. Journal of Advances in Modeling Earth Systems. https://doi.org/10.1029/2018MS001369

Mauritsen, T., Bader, J., Becker, T., Behrens, J., Bittner, M., Brokopf, R., et al. (2019). Developments in the MPI-M Earth System Model version 1.2 (MPI-ESM1.2) and its response to increasing CO2. Journal of Advances in Modeling Earth Systems. https://doi.org/10.1029/2018MS001400

Sellar, A. A., Walton, J., Jones, C. G., Wood, R., Luke Abraham, N., Andrejczuk, M., et al. (2020). Implementation of U.K. Earth System Models for CMIP6. Journal of Advances in Modeling Earth Systems. https://doi.org/10.1029/2019MS001946

Scaife, A. A., & Smith, D. (2018). A signal-to-noise paradox in climate science. npj Climate and Atmospheric Science. https://doi.org/10.1038/s41612-018-0038-4

Smith, D. M., Eade, R., Scaife, A. A., Caron, L. P., Danabasoglu, G., DelSole, T. M., et al. (2019). Robust skill of decadal climate predictions. Npj Climate and Atmospheric Science. https://doi.org/10.1038/s41612-019-0071-y

Solaraju-Murali, B., Gonzalez-Reviriego, N., Caron, L.P., Ceglar, A., Toreti, A., Zampieri, M., et al. (2021). Multi-annual prediction of drought and heat stress to support decision making in the wheat sector. npj Climate and Atmospheric Science, 4(1), pp.1-9. https://doi.org/10.1038/s41612-021-00189-4

3.9 Case #9: Water use impact simulations and projections under 2K global warming.

3.9.1 Practical question posed by stakeholders

The distribution of surface water and the availability of groundwater resources is not just determined by climatic and hydrological processes, but also heavily impacted by human water use and interventions. Considering an ever-growing population, leading to increasing food, energy and production demands relying on sufficient water resources, results in widespread impacts on the supply of water (Wada et al., 2013, 2014, 2016; Flörke et al., 2013). By additionally considering potential water shortages (or excess) arising from recent and anticipated climate change, a reliable water supply is largely at risk in regions with large water demand as well as regions likely to experience drying climatic conditions (e.g., Greve et al., 2018). Under these conditions, water demand is often met through water extractions at the expense of environmental flows and water-dependent ecosystems or through increasing abstraction of non-renewable groundwater resources. The nexus of water-climate-human interactions calls for more holistic approaches considering both climatic and socio-economic pressures to assess their distinct as well as combined impact on the availability and accessibility of water resources, and on the occurrence and intensity of hydrological extremes, such as floods and droughts. It is, therefore, essential to provide a more holistic assessment of anticipated river flows and their sensitivities to different water use assumptions under conditions of ongoing global warming.

3.9.2 General strategy used to solve the question

We aim to address these issues using a high resolution, large-scale hydrological impact model (Burek et al., 2020) forced by a novel set of pseudo-global warming (PGW) experiments (Prein et al., 2017; Brogli et al., 2019). PGW simulations resemble historical weather patterns and events under conditions of 2K (Kelvin) global warming by perturbing historical, reanalysis-driven regional climate simulations. The PGW simulations used here (within the period 1981-2010) are based on the RACMO regional 0.11° spatial resolution within a western European domain. In the reference experiment, RACMO is forced at the boundaries by (i) unperturbed ERA5 reanalysis data, while in the pseudo-global warming experiment, (ii) the forcing data consist of perturbed reanalysis data. We argue that, given the resemblance of historical weather patterns and events in the perturbed runs, the PGW experiments provide a unique opportunity to assess the impact of current water withdrawals under conditions of 2K global warming. We further argue that using unperturbed and perturbed regional climate model output as forcing provides a storyline-driven and end user-focused perspective on water impact assessments. Nonetheless, it is essential to bear in mind that PGW experiments are highly dependent on the modelling and experimental setup, therefore requiring a critical consideration and interpretation of any underlying uncertainties.

3.9.3 EUCP data and methods used in the case study, including EUCP specific advances

We use the Community Water Model (CWatM, Burek et al., 2020), a state-of-the-art large-scale rainfall-runoff and channel routing water resources model partly developed within EUCP. CWatM operates at grid-scale with a high spatial resolution of 5’ (ca. 0.08°) and daily temporal resolution. CWatM is process-based and used to quantify water availability, human water withdrawals of different sectors (industry, domestic, agriculture), and the effects of water infrastructure, including reservoirs, groundwater pumping and irrigation canals. The model is calibrated and validated using time series of observed discharge from 363 gauging stations across Europe. We perform simulations by adjusting historical water withdrawals to different relative levels under PGW conditions (ranging between +/- 50% of historic water withdrawals), thereby providing an ad hoc and simplified representation of multiple, possible future water management scenarios. As a sufficient supply of water is often most critical under low flow conditions, we particularly focus on the lower tail of the distribution of daily discharge. That enables us to directly identify the sensitivity of projected changes in average and low flow discharge conditions against relative changes in water withdrawals (in terms of historical water withdrawals). Assessing average and low flow sensitivities further provides insights into adaptation and mitigation potentials, guiding the design of efficient, sustainable, and robust water management interventions.

3.9.4 Results and discussion

Fig.3.12. Sensitivity of mean discharge and low flows under PGW conditions to relative changes in water withdrawals at grid scale (1st row) and at basin scale (2nd row). The scale shows relative declines in (left column) average discharge (middle) Q10p (flows at the 10th percentile of the daily discharge time series), and (right) Q1p (1st percentile) corresponding to a 10% increase in water withdrawals. Grid cells and basins with average discharge < 10 m3/s are not shown (dark gray).

The storyline-based experimental adjustment of historic water withdrawals under PGW conditions enables an assessment of the sensitivity of average discharge and low flows to changing water withdrawals. We have here performed 11 hydrological simulations by ad-hoc adjusting water withdrawals between 50% and 150% of historic water withdrawals. That range represents differences that can occur when applying different scenarios of future water withdrawals across developed regions, such as Europe. In fact, across Southern Europe, even increases in water withdrawals beyond 150% can occur under more pessimistic scenarios, while decreases in water withdrawals might occur across Central Europe under more optimistic scenarios.

The relative sensitivity to increasing water withdrawals is regionally different (see Fig. 3.12), and, to a large extent, depends on the amount of upstream water withdrawals. Low flow sensitivities are thus highest in regions with large (upstream) water withdrawals (e.g., Central Europe) and can reach up to parity resulting in decreases of 10% in low flows per 10% increase in water withdrawals. Such high sensitivities are primarily located in upstream areas of Central European rivers (e.g., Rhine, Meuse, Seine) in France, Benelux, and Germany. Relative sensitivities in average discharge are, however, relatively small in comparison to low flow sensitivities. The response to varying levels of water withdrawals (within the range of +/- 50% of historic water withdrawals) further exceeds the climate change response of 2K global warming in average and low flows across many parts of Central and Western Europe. Hence, assuming increases in water withdrawals of 50% or less can regionally double the climate-only response. If differences of this magnitude also exist between water use scenarios, identified changes in low flow conditions can either be neutralized or amplified, thereby increasing uncertainties, and hindering robust water management assessments.

Our results show that quantitative assessments of low flows under future warming are impacted by changing future water withdrawals across highly populated and industrialized regions. Therefore, including water withdrawals in hydrological impact assessments is of utmost importance to communicate the associated broad range of uncertainties. Assessments of climate change impacts in near-natural catchments provide only part of the anticipated response and do not necessarily reflect changes experienced within heavily managed river basins, where climate change assessments for adaptation are needed most. Our results also highlight potentials to manage climate change impacts on river flow, especially within the most critical periods of the year. Regions of substantial low flow sensitivity to water withdrawals will benefit most from coordinated efforts to reduce water withdrawals at regional, national and transnational scales.

References

Brogli, R., Kröner, N., Sørland, S.L., Lüthi, D. and Schär, C. (2019). The Role of Hadley Circulation and Lapse-Rate Changes for the Future European Summer Climate. J. Climate, 32, 385–404, https://doi.org/10.1175/JCLI-D-18-0431.1

Burek, P., Y. Satoh, T. Kahil, T. Tang, P. Greve, M. Smilovic, L. Guillaumot, and Y. Wada. (2019). “Development of the Community Water Model (CWatM v1.04) A High-Resolution Hydrological Model for Global and Regional Assessment of Integrated Water Resources Management.” Geoscientific Model Development, August, 1–49. https://doi.org/10.5194/gmd-2019-214.

Flörke, M., E. Kynast, I. Bärlund, S. Eisner, F. Wimmer, and J. Alcamo. (2013). “Domestic and Industrial Water Uses of the Past 60 Years as a Mirror of Socio-Economic Development: A Global Simulation Study.” Global Environmental Change 23 (1): 144–156. https://doi.org/10.1016/j.gloenvcha.2012.10.018.

Greve, P., T. Kahil, J. Mochizuki, T. Schinko, Y. Satoh, P. Burek, G. Fischer, et al. (2018). “Global Assessment of Water Challenges under Uncertainty in Water Scarcity Projections.” Nature Sustainability 1 (9): 486–94. https://doi.org/10.1038/s41893-018-0134-9.

Prein, A., Rasmussen, R., Ikeda, K. et al. The future intensification of hourly precipitation extremes. Nature Clim Change 7, 48–52 (2017). https://doi.org/10.1038/nclimate3168

Wada, Y., D. Wisser, and M. F. P. Bierkens. (2014). “Global Modeling of Withdrawal, Allocation and Consumptive Use of Surface Water and Groundwater Resources.” Earth Syst. Dynam. 5 (1): 15–40. https://doi.org/10.5194/esd-5-15-2014.

Wada, Y., L. P. H. van Beek, N. Wanders, and M. F. P. Bierkens. (2013). “Human Water Consumption Intensifies Hydrological Drought Worldwide.” Environ. Res. Lett. 8 (3): 034036. https://doi.org/10.1088/1748-9326/8/3/034036.

Wada, Y., I. E. M. de Graaf, and L. P. H. van Beek. (2016). “High-Resolution Modeling of Human and Climate Impacts on Global Water Resources.” Journal of Advances in Modeling Earth Systems 8 (2): 735–63. https://doi.org/10.1002/2015MS000618.

3.10 Case #10: Future changes in hurricane occurrence in the Caribbean.

3.10.1 Practical question posed by stakeholders

Besides the European continent the European Union counts nine outermost regions. Ideally, developments in EU projects enable future climate hazard outlooks for these outermost regions as well. The regions are studied less frequently and have limited observational records of precipitation, river flows etc available. In this study we assessed the value of high-resolution climate data for estimating potential changes in hurricane occurrence for the Caribbean Islands Martinique, Saint-Martin and the Dominican Republic. The Caribbean islands are located in an area prone to hurricanes. These hurricanes cause severe damage to the vulnerable islands. For example Hurricane Irma, a severe Category 5 storm, hit Sint-Martin in 2017. 60% of the buildings were totally uninhabitable and the losses were estimated at 3.5 billion Euros. Future climate change may affect hurricane frequency and severity and will cause Sea Level Rise (SLR). High-resolution climate simulations that capture the hurricanes well are only limitedly available. For this study we had access to CP-RCM based Pseudo-Global Warming (PGW) simulations performed by KNMI.

3.10.2 General strategy used to solve the question

To assess the future changes in hurricane occurrence we developed a modeling chain. This modelling chain takes PGW simulations for the historic and future hurricane season (June-Oct) and ERA5 wave data (historic) as input to the Global Tide and Storm Surge model (GTSM; Muis et al., 2020). HCLIM is a regional convection permitting climate modelling system based on the ALADIN–HIRLAM numerical weather prediction system (Belusic et al., 2019). The GTSM results form the coastal boundary condition for the SFINCS model. Sea level rise was added based on global IPCC estimates. The discharges and effective precipitation calculated with the hydrological wflow_sbm model are input for the Super-Fast Inundation of CoastS model (SFINCS; Leijnse et al., 2020) that calculates flood maps for the current and future climate. These flood maps are input to the flood impact module (FIAT; Slager et al., 2016) to assess future flood losses. Due to the limited length of the time-series and the fact that hurricanes do not always occur at the same location it was not possible to perform a full statistical analysis, rather a story-line approach was followed.

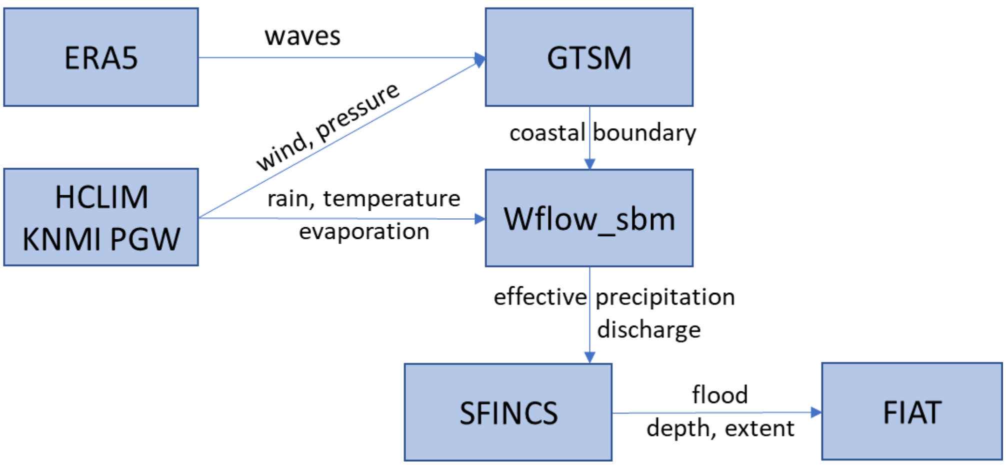

Fig.3.13. overview of the modelling chain employed to assess flood impacts for the current and future climate.

3.10.3 EUCP data and methods used in the case study, including EUCP specific advances

The main advances made are:

- The availability of high-resolution convection permitting HCLIM climate model data produced by consortium partners from WP3 for the Caribbean hurricane season;
- The development of an integrated modelling chain that incorporates coastal, fluvial and pluvial flooding and impact based on these high-resolution climate model data.

3.10.4 Results and discussion

The main results are the flood impact maps. An example is given, showing the damage per grid cell in USD for hurricane Harvey over Martinique. This map shows the historic damage, the damage for PGW alone and PGW combined with sea level rise (SLR).

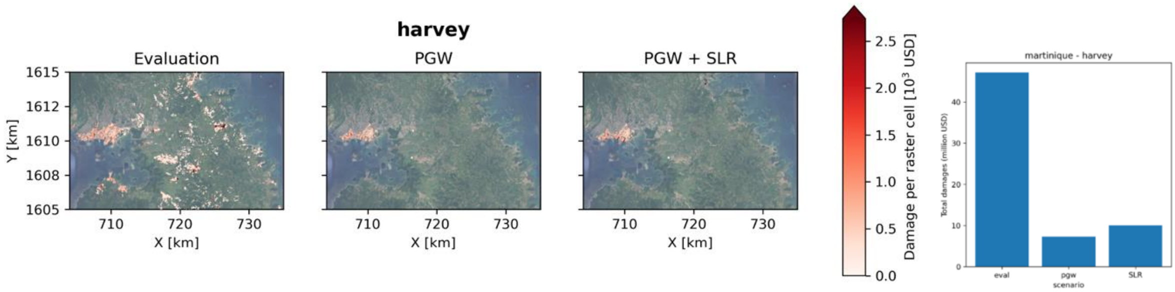

Fig.3.14. Estimated damage for Hurricane Harvey over Maritnique for the evaluation, PGW and PGW+SLR runs.

For this Hurricane the severity seems to decrease. Unfortunately it is not possible to quantify this change and its significance. We only have 10 years of data and could only capture a few hurricanes passing over part of the islands. Although a PGW experiment should represent the same atmospheric condition under a certain degrees-warming the Hurricanes tend to slightly change their tracks making a different landfall. Therefore the results are more illustrative than quantitative and due to the shifts in tracks a storyline approach is also not possible. We decided to do this evaluation for a couple of islands and a couple of storms to also show the uncertainties related to the future projections. Possibly a flood impact analysis for all Caribbean Islands for the full 10-years would provide enough regionalized information to draw conclusions, yet this requires significantly more time. Another option for a proper statistical analysis would either be longer HCLIM simulations or an ensemble of HCLIM simulations. Strength and severity of future storms could then also be analyzed from changes in wind and pressure patterns.

Further improvements to the flood modeling can be achieved by year round HCLIM simulations, now the historic ERA5 driven simulations were used for obtaining the initial conditions at the start of the historic and future hurricane season. Furthermore, in data rich areas improvements can be made by incorporating local measurements of the coastal bathymetry and digital elevation model, meteorological/hydrological observations for model calibration and socio-economic data for the impact modeling.

References

La Croix (in French). "Irma sème 'l'apocalypse' à Saint-Barth et Saint-Martin, au moins 4 morts".Agence France-Presse. September 7, 2017. Archived from the original on September 7, 2017. Retrieved September 7, 2017.

Muis, S., Apecechea, M. I., Dullaart, J., de Lima Rego, J., Madsen, K. S., Su, J., ... & Verlaan, M. (2020). A high-resolution global dataset of extreme sea levels, tides, and storm surges, including future projections. Frontiers in Marine Science, 7, 263.

Leijnse, T., van Ormondt, M., Nederhoff, K., & van Dongeren, A. (2021). Modeling compound flooding in coastal systems using a computationally efficient reduced-physics solver: Including fluvial, pluvial, tidal, wind-and wave-driven processes. Coastal Engineering, 163, 103796.

Slager, K., Burzel, A., Bos, E., De Bruikn, K., Wagenaar, D. J., Winsemius, H. C., ... & Van der Doef, M. (2016). User Manual Delft-FIAT version 1.

3.11 Case #11: Urban and flash flooding.

3.11.1 Practical question posed by stakeholders

Extreme precipitation can cause severe local flooding especially when it concerns urban flooding or flash floods. Observational records have shown increases in the intensity of extreme rainfall over the past decades, mostly for short sub-daily durations (Förster and Thiele, 2020). In the future these changes are expected to continue and may cause even more damage. The new generation of convection-permitting regional climate models (CP-RCMs) can potentially enhance our understanding of changes in rainfall extremes as they can simulate the hourly statistics and diurnal cycle of the modeled rainfall as well as the size and shape of rainfall fields (Ban et al., 2021). Within EUCP we focussed on two applications of CP-RCM data, (1) urban flooding in European cities and (2) flash flooding in the Alps.

3.11.2 General strategy used to solve the question

Unfortunately the 10-years of available CP-RCM data is very limited to conduct extreme value analysis for extreme rainfall events where one is interested in events with return periods of 10-years or more. We investigated the potential of Meta-statistical analysis (MEV; Marani and Ignaccolo, 2015). MEV is a novel method in extreme value analysis that considers ordinary events as well as the extremes to overcome the problem of a limited sample size. In addition, we applied a regional frequency analysis for flash flood occurrence in the Alps. This regional approach allows for using the high spatial resolution by grouping the data of all individual grid cells from CP-RCM simulations over the Alpine domain to assess future flash flooding (Zander et al., 2021).

3.11.3 EUCP data and methods used in the case study, including EUCP specific advances

The main advances made are:

- The use of the available high-resolution convection permitting climate model data produced by consortium partners from WP3 over the Alpine domain;
- Advanced regionalized and meta-statistical analysis to overcome limited CP-RCM time-series length.

3.11.4 Results and discussion

MEV: The MEV method was tested for different sample sizes from a longer observational record. MEV was indeed more advantageous than traditional extreme value analysis methods in the case of small sample data, yet the shape and position of the MEV distribution is highly influenced by the selected events / period. Fig.3.15 shows the extreme value distributions derived when using only events from 1939 and when using only events from 1953. The long-term annual maxima are shown in gray diamonds in both graphs. The MEV distributions clearly shift when a period with less or more extreme events is used. When the period is lengthened the distributions tend to converge. The full analysis conducted for the CP-RCM climate data showed that over Germany by mid-century changes in hourly precipitation extremes are not evident, while by the end of century hourly precipitation extremes increase significantly. Overall MEV seems a promising method to be further investigated and to be applied at the urban scale in the future.

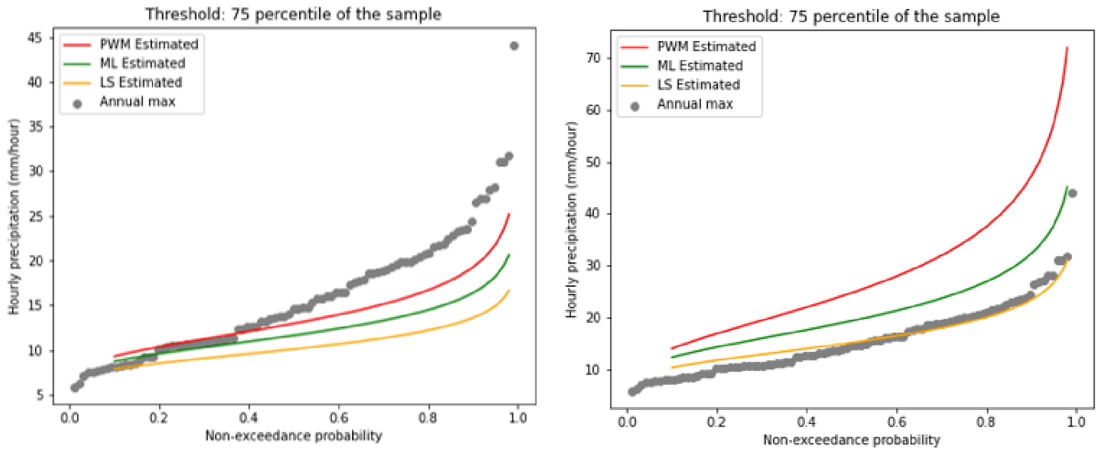

1939 1953

Fig. 3.15. Historica Meta-statistical extreme value distributions derived from events for the year 1939 and 1953. Both graphs have the same observed annual maxima (gray diamonds) as reference. Results are shown for different fitting methods weighted moment (PWM), maximum likelihood (ML), and least square (LS).

RFA: We also investigated a regionalization method over the Alpine domain to assess future flash flooding (Zander et al., 2021). This work was rather promising and has been submitted for publication. Time-series from all grid-cells for the river basins in the Alpine domain were combined. The number of days on which the estimated flash flood threshold (0.5 cubs/sec) for peak specific discharge was reached or exceeded for the Future and Current Climate simulations for summer and autumn was quantified. In summer there are more days with threshold exceedances in the Current Climate scenario while in autumn we see the opposite with more threshold exceedances in the Future Climate scenario. There are some regional differences.

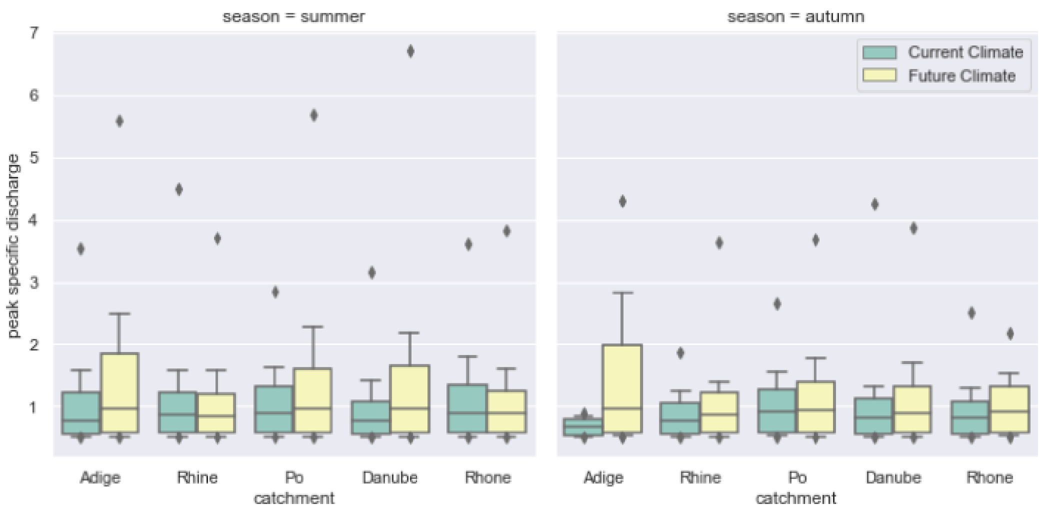

Fig.3.16. Boxplots for maximal daily specific discharge exceeding the 0.5 m3 s −1km−2 specific threshold for summer (JJA) and autumn (SON) for the Current Climate and Future Climate simulation.

Conclusion: We found two methods that hold potential to use the CP-RCM datasets of decadal length for extreme value analysis and to quantify future changes in urban and flash flood risk. Yet in the end these analyses would greatly benefit from lengthened or ensembles of CP-RCM simulations. Currently computer power is an important bottleneck both for the climate simulations and the processing of the data.

References

Ban et al., 2021. The first multi-model ensemble of regional climate simulations at kilometer-scale resolution, part i: evaluation of precipitation. Climate Dynamics, https://doi.org/10.1007/s00382-021-05708-w.

Förster, K., & Thiele, L. B. (2020). Variations in sub-daily precipitation at centennial scale. npj Climate and Atmospheric Science, 3(1), 1-7.

Zander. M.J., Viguurs, P.J., Sperna Weiland, F.C. and A.H. Weerts. (2021). Future changes in flash flood frequency and magnitude over the European Alps Weather and Climate Extremes (submitted).

3.12 List peer reviewed articles produced.

Ban et al., 2021. The first multi-model ensemble of regional climate simulations at kilometer-scale resolution, part i: evaluation of precipitation. Climate Dynamics, https://doi.org/10.1007/s00382-021-05708-w.

Bilbao, R., Wild, S., Ortega, P., Acosta-Navarro, J., Arsouze, T., Bretonnière, P.-A., Caron, L.-P., Castrillo, M., Cruz-García, R., Cvijanovic, I., Doblas-Reyes, F. J., Donat, M., Dutra, E., Echevarría, P., Ho, A.-C., Loosveldt-Tomas, S., Moreno-Chamarro, E., Pérez-Zanon, N., Ramos, A., Ruprich-Robert, Y., Sicardi, V., Tourigny, E., and Vegas-Regidor, J. (2021). Assessment of a full-field initialized decadal climate prediction system with the CMIP6 version of EC-Earth, Earth Syst. Dynam., 12, 173–196, https://doi.org/10.5194/esd-12-173-2021

Burek, P., Y. Satoh, T. Kahil, T. Tang, P. Greve, M. Smilovic, L. Guillaumot, and Y. Wada. 2019. "Development of the Community Water Model (CWatM v1.04) A High-Resolution Hydrological Model for Global and Regional Assessment of Integrated Water Resources Management." Geoscientific Model Development, August, 1–49. https://doi.org/10.5194/gmd-2019-214.

Lledó, L., Bellprat, O., Doblas-Reyes, F. J., & Soret, A. (2018). Investigating the effects of Pacific sea surface temperatures on the wind drought of 2015 over the United States. Journal of Geophysical Research: Atmospheres, 123, 4837– 4849. https://doi.org/10.1029/2017JD028019

Tian, T., Yang, S., Karami, M. P., Massonnet, F., Kruschke, T., and Koenigk, T. (2021). Benefits of sea ice initialization for the interannual-to-decadal climate prediction skill in the Arctic in EC-Earth3, Geosci. Model Dev., 14, 4283–4305, https://doi.org/10.5194/gmd-14-4283-2021

Smith, D. M., Eade, R., Scaife, A. A., Caron, L. P., Danabasoglu, G., DelSole, T. M., et al. (2019). Robust skill of decadal climate predictions. Npj Climate and Atmospheric Science. https://doi.org/10.1038/s41612-019-0071-y

Solaraju-Murali, B., Gonzalez-Reviriego, N., Caron, L.P., Ceglar, A., Toreti, A., Zampieri, M., et al. (2021). Multi-annual prediction of drought and heat stress to support decision making in the wheat sector. npj Climate and Atmospheric Science, 4(1), pp.1-9. https://doi.org/10.1038/s41612-021-00189-4

3.13 List planned future publications.

Yu S, Vautard R. A transfer method to estimate hub-height wind speed from 10 meters wind speed based on machine learning. Renewable & Sustainable Energy Reviews.2022 (under review).

Yu S, Vautard R. Attribution of regional winter wind energy drought in Europe. Environment Research Letter. 2022. (to be submitted)

Yu S, Vautard R. Wind energy drought under cold conditions in Europe. 2022. (in progress)

Zander. M.J., Viguurs, P.J., Sperna Weiland, F.C. and A.H. Weerts. Future changes in flash flood frequency and magnitude over the European Alps Weather and Climate Extremes (submitted), 2021.

4. Lessons Learnt and links Built

4.1 Lessons learnt: positive and negative that can be drawn from the experience of the work to date.

1) Large ensemble for the model simulation is essential for extreme statistics and attribution research. High-resolution climate models also hold promise but simulations are currently not long enough for the extreme statistics, which challenges the attribution research at a wind farm site. Thus, it is crucial to explore the long-term high-resolution climate simulations in future research.

2) For the wind power estimation and attribution research, iterative statistical methods and indices should be considered to strengthen the robustness of the estimation and attribution results. Larger weight on more skilful simulations should be given for a more reliable result.

3) Capturing the correct wind variability at local, near site scale is a big challenge for using wind energy. Wind energy assessment using low-resolution models might smooth out extreme-value signals in particular. Therefore, a high-resolution model is crucial for finding wind energy rich locations and site selection for wind farms. However, when using high resolution model simulation results, large ensembles for model simulations should be considered to address structural uncertainty.

4) We predict surface wind speed at multi-annual and multi-seasonal time scales. The main difficulties of this study have been the huge amount of data (sub-daily data from multiple forecast systems over more than 60 years), the short ensemble size for forecast generation (as only a few systems provide sub-daily wind data and only one of them is operational), and how to adapt and communicate the probabilistic information to users (in addition to the interpretation of the skill estimates).

5) We have explored the pluvial hazard risk and risk-mitigation measures over the city of Milan in northern Italy. Here we use a simplified and computationally efficient raster-based model based on a hierarchical filling and spilling algorithm. Results show that high resolution, convection permitting simulations allow to refine the pluvial flood hazard and risk. Nature-based solutions can provide means to mitigating climate risks. Simulation of risk reduction measures and planning of urban green areas challenging in densely developed areas.

6) High performance computing and advances in numerical computing algorithms have made it possible to develop a new generation of flood hazard and risk models and high-resolution exposure mapping.

7) Large ensembles are helpful to achieve more reliable and skillful forecasts in predicting drought conditions on a multi-annual timescale over the global wheat harvest areas.

8) We provide a more holistic assessment of anticipated river flows and their sensitivities to different water use assumptions under conditions of ongoing global warming. Quantitative assessments of low flows under future warming are impacted by changing future water withdrawals across highly populated and industrialized regions.

9) Assessment of the value of high-resolution climate data for estimating potential changes in hurricane occurrence for the Caribbean Islands Martinique, Saint-Martin and the Dominican Republic. Results show that future climate change may affect hurricane frequency and severity and will cause Sea Level Rise. However, we only have 10 years of data and could only capture a few hurricanes

passing over part of the islands. Thus, the results are more illustrative than quantitative and due to the shifts in tracks a storyline approach is also not possible.

10) We found two methods that hold potential to use the CP-RCM datasets of decadal length for extreme value analysis and to quantify future changes in urban and flash flood risk. Yet in the end these analyses would greatly benefit from lengthened or ensembles of CP-RCM simulations. Currently computer power is an important bottleneck both for the climate simulations and the processing of the data.

4.2 Links built with other deliverables, work packages, and synergies and links created with other projects.

There were links built from WP4 with WP3 and WP1 for high resolution simulations and decadal predictions. The cases are inspiring other projects such as the new H2020 XAIDA project on the attribution of climate extremes (this is one of several examples).

5. References

Ban et al., 2021. The first multi-model ensemble of regional climate simulations at kilometer-scale resolution, part i: evaluation of precipitation. Climate Dynamics, https://doi.org/10.1007/s00382-021-05708-w.

Bansal, R. C., Bhatti, T. S., & Kothari, D. P. (2002). On some of the design aspects of wind energy conversion systems. *Energy conversion and management*, *43*(16), 2175-2187.

Bilbao, R., Wild, S., Ortega, P., Acosta-Navarro, J., Arsouze, T., Bretonnière, P.-A., Caron, L.-P., Castrillo, M., Cruz-García, R., Cvijanovic, I., Doblas-Reyes, F. J., Donat, M., Dutra, E., Echevarría, P., Ho, A.-C., Loosveldt-Tomas, S., Moreno-Chamarro, E., Pérez-Zanon, N., Ramos, A., Ruprich-Robert, Y., Sicardi, V., Tourigny, E., and Vegas-Regidor, J. (2021). Assessment of a full-field initialized decadal climate prediction system with the CMIP6 version of EC-Earth, Earth Syst. Dynam., 12, 173–196, https://doi.org/10.5194/esd-12-173-2021.

Boer, G. J., Smith, D. M., Cassou, C., Doblas-Reyes, F., Danabasoglu, G., Kirtman, B., Kushnir, Y., Kimoto, M., Meehl, G. A., Msadek, R., Mueller, W. A., Taylor, K. E., Zwiers, F., Rixen, M., Ruprich-Robert, Y., and Eade, R. (2016). The Decadal Climate Prediction Project (DCPP) contribution to CMIP6, Geosci. Model Dev., 9, 3751–3777, https://doi.org/10.5194/gmd-9-3751-2016

Boucher, O., Servonnat, J., Albright, A. L., Aumont, O., Balkanski, Y., & Bastrikov, V., et al. (2020). Presentation and evaluation of the IPSL-CM6A-LR climate model. Journal of Advances in Modeling Earth Systems, 12, e2019MS002010. https://doi.org/10.1029/2019MS002010

Brogli, R., Kröner, N., Sørland, S.L., Lüthi, D. and Schär, C. (2019): The Role of Hadley Circulation and Lapse-Rate Changes for the Future European Summer Climate. J. Climate, 32, 385–404, https://doi.org/10.1175/JCLI-D-18-0431.1

Burek, P., Y. Satoh, T. Kahil, T. Tang, P. Greve, M. Smilovic, L. Guillaumot, and Y. Wada. 2019. "Development of the Community Water Model (CWatM v1.04) A High-Resolution Hydrological Model for Global and Regional Assessment of Integrated Water Resources Management." Geoscientific Model Development, August, 1–49. https://doi.org/10.5194/gmd-2019-214.

Cherchi, A., Fogli, P. G., Lovato, T., Peano, D., Iovino, D., Gualdi, S., et al. (2018). Global Mean Climate and Main Patterns of Variability in the CMCC-CM2 Coupled Model. Journal of Advances in Modeling Earth Systems. https://doi.org/10.1029/2018MS001369

DelSole, T., & Tippett, M. K. (2016). Forecast Comparison Based on Random Walks, Monthly Weather Review, 144(2), 615-626. https://doi.org/10.1175/MWR-D-15-0218.1

DNV, G. (2018). Energy Transition Outlook 2018: A global, regional forecast of the energy transition to 2050. Last accessed Dec, 17, 2018.

Dubus, L. (2010). Practises, needs and impediments in the use of weather/climate information in the electricity sector, in Management of Weather and Climate Risk for the Energy Sector, A. Troccoli, ed., NATO Science Series, Springer Academic Publisher, ISBN 97890-481-3691-9.

Efron, B., & Tibshirani, R. J. (1994). An introduction to the bootstrap. CRC press.

Eyring, V., Bony, S., Meehl, G. A., Senior, C. A., Stevens, B., Stouffer, R. J., and Taylor, K. E. (2016). Overview of the Coupled Model Intercomparison Project Phase 6 (CMIP6) experimental design and organization, Geosci. Model Dev., 9, 1937–1958, https://doi.org/10.5194/gmd-9-1937-2016

Flörke, M., E. Kynast, I. Bärlund, S. Eisner, F. Wimmer, and J. Alcamo. 2013. "Domestic and Industrial Water Uses of the Past 60 Years as a Mirror of Socio-Economic Development: A Global Simulation Study." Global Environmental Change 23 (1): 144–156. https://doi.org/10.1016/j.gloenvcha.2012.10.018.

Förster, K., & Thiele, L. B. (2020). Variations in sub-daily precipitation at centennial scale. npj Climate and Atmospheric Science, 3(1), 1-7.

Greve, P., T. Kahil, J. Mochizuki, T. Schinko, Y. Satoh, P. Burek, G. Fischer, et al. 2018. "Global Assessment of Water Challenges under Uncertainty in Water Scarcity Projections." Nature Sustainability 1 (9): 486–94. https://doi.org/10.1038/s41893-018-0134-9.

Hersbach, H., Bell, B., Berrisford, P., Hirahara, S., Horányi, A., Muñoz-Sabater, J., ... & Thépaut, J. N. (2020). The ERA5 global reanalysis, QJ Roy. Meteor. Soc., 146, 1999–2049.

International Energy Agency (2021). Spain 2021, Energy Policy Review. Country report. May 2021. Retrieved from https://www.iea.org/reports/spain-2021

Hu, S., Yan, D., Cui, Y., & Guo, S. (2016). Urban residential heating in hot summer and cold winter zones of China—Status, modeling, and scenarios to 2030. Energy Policy, 92, 158-170.

Jacob, D., and Coauthors, (2014): EURO-CORDEX: New high-resolution climate change projections for European impact research. Reg. Environ. Change, 14, 563–578, doi:10.1007/s10113-013-0499-2.

Jung J, Broadwater R P. Current status and future advances for wind speed and power forecasting. Renewable and Sustainable Energy Reviews, 2014, 31: 762-777.

Kharin, V. V., & Zwiers, F. W. (2003). On the ROC Score of Probability Forecasts, Journal of Climate, 16(24), 4145-4150. https://doi.org/10.1175/1520-0442(2003)016%3C4145:OTRSOP%3E2.0.CO;2

La Croix (in French). "Irma sème 'l'apocalypse' à Saint-Barth et Saint-Martin, au moins 4 morts".Agence France-Presse. September 7, 2017. Archived from the original on September 7, 2017. Retrieved September 7, 2017.

Leijnse, T., van Ormondt, M., Nederhoff, K., & van Dongeren, A. (2021). Modeling compound flooding in coastal systems using a computationally efficient reduced-physics solver: Including fluvial, pluvial, tidal, wind-and wave-driven processes. Coastal Engineering, 163, 103796.

Li, J., Lv, Q., Zhang, M., Wang, T., Kawamoto, K., Chen, S., & Zhang, B. (2017). Effects of atmospheric dynamics and aerosols on the fraction of supercooled water clouds. Atmospheric Chemistry and Physics, 17(3), 1847-1863.

Lledó, L., Bellprat, O., Doblas-Reyes, F. J., & Soret, A. (2018). Investigating the effects of Pacific sea surface temperatures on the wind drought of 2015 over the United States. Journal of Geophysical Research: Atmospheres, 123, 4837– 4849. https://doi.org/10.1029/2017JD028019

Mauritsen, T., Bader, J., Becker, T., Behrens, J., Bittner, M., Brokopf, R., et al. (2019). Developments in the MPI-M Earth System Model version 1.2 (MPI-ESM1.2) and its response to increasing CO2. Journal of Advances in Modeling Earth Systems. https://doi.org/10.1029/2018MS001400

McVicar TR, Roderick ML, Donohue RJ, Li LT, Van Niel TG, Thomas A, Grieser J, Jhajharia D, Himri Y, Mahowald NM, Mescherskaya AV, Kruger AC, Rehman S, Dinpashoh Y. (2012). Global review and synthesis of trends in observed terrestrial near-surface wind speeds: implications for evaporation. J. Hydrol. 416–417: 182–205. https://doi.org/10.1016/j.jhydrol.2011.10.024.

Meyer, G. (2015). US clean energy suffers from lack of wind, Financial Times. 1 September 2015. Retrieved from https://www.ft.com/content/b967b6d4-5058-11e5-8642-453585f2cfcd.

Muis, S., Apecechea, M. I., Dullaart, J., de Lima Rego, J., Madsen, K. S., Su, J., ... & Verlaan, M. (2020). A high-resolution global dataset of extreme sea levels, tides, and storm surges, including future projections. Frontiers in Marine Science, 7, 263.

Müller, W. A., Jungclaus, J. H., Mauritsen, T., Baehr, J., Bittner, M., Budich, R., et al. (2018). A higher-resolution version of the Max Planck Institute Earth System Model (MPI-ESM1.2-HR). Journal of Advances in Modeling Earth Systems, 10, 1383– 1413. https://doi.org/10.1029/2017MS001217.

Kharin, V. V. and Zwiers, F. W. (2003). On the ROC Score of Probability Forecast. Journal of Climate. https://doi.org/10.1175/1520-0442(2003)016%3C4145:OTRSOP%3E2.0.CO;2

Philip, S., Kew, S., van Oldenborgh, G. J., Otto, F., Vautard, R., van der Wiel, K., ... & van Aalst, M. (2020). A protocol for probabilistic extreme event attribution analyses. Advances in Statistical Climatology, Meteorology and Oceanography, 6(2), 177-203.

Prein, A., Rasmussen, R., Ikeda, K. et al. The future intensification of hourly precipitation extremes. Nature Clim Change 7, 48–52 (2017). https://doi.org/10.1038/nclimate3168

Ribes, A., Boé, J., Qasmi, S., Dubuisson, B., Douville, H., & Terray, L. (2022). An updated assessment of past and future warming over France based on a regional observational constraint. Earth System Dynamics Discussions, 1-29.

Scaife, A. A., & Smith, D. (2018). A signal-to-noise paradox in climate science. npj Climate and Atmospheric Science. https://doi.org/10.1038/s41612-018-0038-4

Slager, K., Burzel, A., Bos, E., De Bruikn, K., Wagenaar, D. J., Winsemius, H. C., ... & Van der Doef, M. (2016). User Manual Delft-FIAT version 1.

Smith, D. M., Eade, R., Scaife, A. A., Caron, L. P., Danabasoglu, G., DelSole, T. M., et al. (2019). Robust skill of decadal climate predictions. Npj Climate and Atmospheric Science. https://doi.org/10.1038/s41612-019-0071-y

Solaraju-Murali, B., Gonzalez-Reviriego, N., Caron, L.P., Ceglar, A., Toreti, A., Zampieri, M., et al. (2021). Multi-annual prediction of drought and heat stress to support decision making in the wheat sector. npj Climate and Atmospheric Science, 4(1), pp.1-9. https://doi.org/10.1038/s41612-021-00189-4.

Roderick ML, Rotstayn LD, Farquhar GD, Hobbins MT. (2007). On the attribution of changing pan evaporation. Geophys. Res. Lett. 34(17): L17403.

Sellar, A. A., Walton, J., Jones, C. G., Wood, R., Luke Abraham, N., Andrejczuk, M., et al. (2020). Implementation of U.K. Earth System Models for CMIP6. Journal of Advances in Modeling Earth Systems. https://doi.org/10.1029/2019MS001946

Stott, P. A., Christidis, N., Otto, F. E., Sun, Y., Vanderlinden, J. P., van Oldenborgh, G. J., ... & Zwiers, F. W. (2016). Attribution of extreme weather and climate‐related events. Wiley Interdisciplinary Reviews: Climate Change, 7(1), 23-41.

Tian, T., Yang, S., Karami, M. P., Massonnet, F., Kruschke, T., and Koenigk, T. (2021). Benefits of sea ice initialization for the interannual-to-decadal climate prediction skill in the Arctic in EC-Earth3, Geosci. Model Dev., 14, 4283–4305, https://doi.org/10.5194/gmd-14-4283-2021.

Vautard R, Cattiaux J, Yiou P, Thépaut JN, Ciais P. (2010). Northern hemisphere atmospheric stilling partly attributed to an increase in surface roughness. Nat. Geosci. 3(11): 756–761. https://doi.org/10.1038/ngeo979.

Von Storch, H. and Zwiers, F. W. (2001). Statistical Analysis in Climate Research. Cambridge: Cambridge University Press. https://doi.org/10.1017/CBO9780511612336.

Wada, Y., L. P. H. van Beek, N. Wanders, and M. F. P. Bierkens. 2013. "Human Water Consumption Intensifies Hydrological Drought Worldwide." Environ. Res. Lett. 8 (3): 034036. https://doi.org/10.1088/1748-9326/8/3/034036.

Wada, Y., D. Wisser, and M. F. P. Bierkens. 2014. "Global Modeling of Withdrawal, Allocation and Consumptive Use of Surface Water and Groundwater Resources." Earth Syst. Dynam. 5 (1): 15–40. https://doi.org/10.5194/esd-5-15-2014.

Wada, Y., I. E. M. de Graaf, and L. P. H. van Beek. 2016. "High-Resolution Modeling of Human and Climate Impacts on Global Water Resources." Journal of Advances in Modeling Earth Systems 8 (2): 735–63. https://doi.org/10.1002/2015MS000618.

List of Tables

Table 3.1: List of remarkable cases used in EUCP

Table 3.2: Forecast systems that provide sub-daily surface wind speed data contributing to the CMIP6/DCPP and their specifications (available simulations at the time of the study).

List of Figures

Fig.3.1. Seasonal cycle of surface wind based on observations during 1988-2017. The operational period (green) wind weaker than assessment period (blue).

Fig.3.2. Changes in return values and return periods of load factor for model ensemble. The black horizontal line shows the return value corresponding to the 10-years return period during 2000 to 2029. Dots represent median of consecutive sorted return period/values model values from 10000 bootstrap estimations, together with 5%-95% confidence intervals (dashed lines).

Fig.3.3. Boxplot and geographical distribution of (a,b) the return values corresponding to the 10-years events during 2000 to 2029 in each countries, which were referred as threshold; (c,d) the risk ratios between 1971-2000 and 2000-2029, and (e,f) the risk ratios between 2000-2029 and 2041-2069. The probability of low wind energy winter was increased when risk ratios were larger than 1. For boxplot (c,e), the red dot shows the median of all the grids in this region; the vertical bar shows the small uncertainty interval of the median. The 5% and 95% of the medians show the uncertainty interval.

Fig.3.4. The (a) risk ratio and (b) threshold based on three different experiments. When the risk ratio <1, the low wind energy event is more frequent in the earlier climate period. The threshold is the return value of indicator of 10-years events during the current climate. The previous is from 1971 to 2000, the current climate is from 2000 to 2029, and the future climate is from 2041 to 2069.

Fig.3.5. Geographical distribution of the (a-b) annual mean value of wind speed in 2004 and the (c-d) daily mean value of wind speed in 17-Dec-2004. The left figures show the wind speed from the high resolution model and the right figures show that from the low resolution model. (e) Compared the seasonal cycle of w100 based on two different models.

Fig.3.6. Multi-model skill in predicting the surface wind speed for the forecast years 1-5.

Fig.3.7. EC-Earth3-i4 skill in predicting the surface wind speed for the forecast years 1-5.

Fig.3.8. EC-Earth3-i4 forecast of the surface wind speed for the forecast years 1-5 over Indiana, USA.

Fig.3.9. Expected direct tangible damages due to pluvial flooding in Milan under the historical, RCP 8.5 mid-century, and RCP 8.5 late-century climate scenarios. On the left, the expected damage – probability curve. On the right, the expected annual damage (EAD) for each climate scenario.

Fig.3.10. Cesenatico: Expected Annual Damage (EAD) according to undefended scenario up to 2100 [left]; EAD reduction thanks to hazard mitigation offered by the coastal barrier [right].

Fig.3.11: (a) Wheat harvest months that are used as a target month to study SPEI6. (b) Most likely tercile category (below-normal, normal and above-normal) of SPEI6 over the global wheat harvesting

regions, in which the colored grids show the category with the highest probability of occurrence. (c) Ranked Probability Skill Score, RPSS of SPEI6 forecast averaged over years 1–5, during the wheat harvest month in each area, for the period 1961–2014.

Fig.3.12. Sensitivity of mean discharge and low flows under PGW conditions to relative changes in water withdrawals at grid scale (1st row) and at basin scale (2nd row). The scale shows relative declines in (left column) average discharge (middle) Q10p (flows at the 10th percentile of the daily discharge time seriese), and (right) Q1p (1st percentile) corresponding to a 10% increase in water withdrawals. Grid cells and basins with average discharge < 10 m3/s are not shown (dark gray).

Fig.3.13. overview of the modelling chain employed to assess flood impacts for the current and future climate

Fig.3.14. Estimated damage for Hurricane Harvey over Maritnique for the evaluation, PGW and PGW+SLR runs

Fig. 3.15. Historica Meta-statistical extreme value distributions derived from events for the year 1939 and 1953. Both graphs have the same observed annual maxima (gray diamonds) as reference. Results are shown for different fitting methods weighted moment (PWM), maximum likelihood (ML), and least square (LS).

Fig.3.16. Boxplots for maximal daily specific discharge exceeding the 0.5 m3 s −1km−2 specific threshold for summer (JJA) and autumn (SON) for the Current Climate and Future Climate simulation.